

LONG WAVELENGTH SOLITARY WAVES IN HERTZIAN CHAINS

MICHELLE PRZEDBORSKI¹ AND STEPHEN C. ANCO²

¹DEPARTMENT OF PHYSICS
BROCK UNIVERSITY
ST. CATHARINES, ON L2S3A1, CANADA

²DEPARTMENT OF MATHEMATICS AND STATISTICS
BROCK UNIVERSITY
ST. CATHARINES, ON L2S3A1, CANADA

ABSTRACT. Properties of solitary waves in weakly pre-compressed Hertzian chains are studied in the long wavelength regime using a well-known continuum model. Several main results are obtained by parameterizing solitary waves in terms of their impulse momentum and their asymptotic amplitude. First, solitary waves with a fixed impulse are shown to comprise a one-parameter family of solutions, and the shape of these solitary waves is shown to be highly sensitive to their wave speed. Second, an explicit approximate formula for their physical height and width is derived. This formula is used to compare the shape of the solitary waves to the shape of Nesterenko's compacton solution having the same impulse momentum. An important conclusion is that solitary waves have a noticeably different shape than the compacton if the speed ratio between the solitary waves and the compacton exceeds approximately 10%. Exact solitary wave solutions are used to illustrate all of these results.

email: mp06lj@brocku.ca, sancoc@brocku.ca

1. INTRODUCTION

There has been considerable interest in the study of one-dimensional chains of discrete macroscopic particles that interact by a power-law contact potential [1–39]. These potentials have the form $V = a\delta^{k+1}$ where $\delta \geq 0$ is the dynamical overlap distance between adjacent particles, a is a constant which depends on their material properties, and $k > 1$ is determined by the geometry of their contact surface [40–42]. In particular, spherical particles have $k = 3/2$ [43].

One of the original motivations was the experimental discovery [1–3] that the dynamical strain in these discrete systems can exhibit solitary waves which are propagating non-dispersive localized pulses. The existence of such waves makes the systems useful for a variety of physical applications related to shock absorption [44–51] and energy localization [52–57].

Experimental and numerical results [18, 58, 59] indicate that the typical wavelength of solitary waves compared to the size of the particles in the discrete system is large enough to allow the use of a nonlinear continuum model for studying analytical properties of the solitary waves. The strongest nonlinearity arises when the discrete system is either uncompressed, with adjacent particles being just in contact, or weakly compressed, with the dynamical overlap δ being approximately at least the size of the initial overlap. These two cases for arbitrary $k > 1$ lead to a continuum model which is given by a highly nonlinear, fourth-order

wave equation [3, 18, 29, 32]. The gradient of solutions corresponds to the dynamical strain in the discrete system, and the spatial asymptotic value of the strain corresponds to the pre-compression in the discrete system. In particular, this asymptotic value is zero for the case when adjacent particles are initially just in contact (corresponding to no pre-compression).

This highly nonlinear wave equation, which we refer to as the long-wavelength Hertzian continuum (LWHC) wave equation, has a well-known explicit solution [1–3] whose gradient is a periodic travelling wave. A single arch of this periodic travelling wave can be cut off in a sufficiently smooth fashion when $1 < k < 5/3$ to yield an exact compact nonlinear wave solution, called a compacton. For $k > 5/3$, the cutoff is singular, which is sometimes not emphasized in the literature. Since the spatial asymptotic amplitude of the compacton is zero, this compacton represents a compact solitary wave in the case corresponding to an uncompressed discrete system.

In the case corresponding to a weakly compressed discrete system, however, the compacton solution does not represent a physical solitary wave solution as it does not have a non-zero asymptotic amplitude. Nevertheless, there is an argument in the literature [18] that claims the compacton should be a close approximation to an actual solitary wave solution, at least in the limit of very small pre-compression. The argument uses a qualitative analysis of the differential equation governing exact travelling wave solutions. In particular, this travelling wave equation can be reduced to a second-order differential equation that is analogous to motion in a potential well, with a free parameter controlling the shape of the potential. Qualitatively, the motion corresponding to the compacton is obtained when the parameter is given by a limiting value in the parameter range for the motions that correspond to the actual solitary waves. However, the shape of the potential undergoes a change at that particular parameter value, and so the question arises as to how closely the compacton approximates the actual solitary waves, especially for parameter values away from the limiting value.

More importantly, since the compacton solution is limited to contact surface geometries with $1 < k < 5/3$, it cannot be used as an approximate solitary wave solution when $k > 5/3$. Contact geometries with $k > 5/3$ occur in several physically interesting discrete systems, particularly when the macroscopic particles in the system have rough contact surfaces [40, 60, 61].

In previous work [62], we have derived an exact quadrature expression for the solitary wave solutions as well as the periodic travelling wave solutions of the LWHC equation for all $k > 1$. We use these expressions in the present paper to examine the properties of the exact solitary wave solutions in the general case $k > 1$, and we compare these solitary waves with the compacton solution in the case $1 < k < 5/3$. This analysis is carried out by fixing a value for the impulse momentum of the solutions, where the impulse momentum is defined by an exact conservation law of the LWHC equation.

We obtain several main results.

First, we show that the impulse momentum for a solitary wave depends on both the wave speed and the asymptotic value of the wave amplitude. Consequently, for any given value of the impulse momentum, a one-parameter family of solitary waves exists, which we write down by an explicit quadrature formula.

Second, we derive an explicit approximate formula for the physical height and width of these solitary waves, holding for a large range of parameter values. This formula shows that

all solitary waves have a width of at least two particle diameters when the Hertz exponent is $1 < k \lesssim 3.5$, which confirms the validity of the continuum model for studying solitary waves.

Third, we show that impulse momentum for the compacton depends only on its wave speed, and so a unique compacton exists for any given value of the impulse momentum. When the impulse momentum is fixed, we show that speed of the solitary waves in the one-parameter family always exceeds the speed of the compacton, and we also show that the shape of these solitary waves is highly sensitive to their wave speed.

Significantly, we find that the solitary waves have a noticeably different shape than the compacton if the speed ratio between the solitary waves and the compacton exceeds approximately 10%.

These results indicate that a continuum system supports solitary waves having the same impulse momentum yet displaying marked different shapes and speeds in comparison to a compacton. The same conclusion will hold for a physical discrete system in the long wavelength regime when $1 < k \lesssim 3.5$.

We illustrate the results for three special cases: $k = 3/2$, $k = 2$, and $k = 3$. The first case is the Hertz exponent for standard contact geometries [43], while the other two cases are Hertz exponents for more complicated contact geometries [60, 63].

The paper is organized as follows. In section 2, we discuss the LWHC equation and its conservation laws for impulse momentum, energy, and momentum. In section 3, we first review the quadrature expression for all exact solitary wave solutions. In the two cases $k = 2$ and $k = 3$, we note that the solitary waves have explicit expressions in terms of elementary functions, which were derived in our previous work. In the case $k = 3/2$, we present an implicit expression for the solitary waves in terms of elliptic functions (for which some details are given in an appendix). This result has not appeared previously in the literature. In section 4, we give the main results. Finally, we make some concluding remarks in section 5.

2. LONG-WAVELENGTH CONTINUUM WAVE EQUATION AND ITS CONSERVATION LAWS

The equations of motion for a one-dimensional homogeneous chain of $N \gg 1$ discrete particles interacting by a general power-law contact potential are given by

$$m\ddot{u}_i = (k + 1)a((\delta_0 + u_{i-1} - u_i)^k - (\delta_0 + u_i - u_{i+1})^k), \quad i = 2, \dots, N - 1 \quad (2.1)$$

in terms of the particle displacements $u_j(t)$, $j = 1, \dots, N$, relative to their initial (equilibrium) positions, where $\delta_0 \geq 0$ is the initial overlap between adjacent particles due to pre-compression of the chain at $t = 0$, and $k > 1$ is determined by the geometry of their contact surface. Here m is the particle mass, and a is a constant which depends on the particles' material properties. The particles at each end of the chain obey similar equations of motion with a different potential that takes into account the boundary conditions. Since we will be interested in the continuum limit, in which $N \rightarrow \infty$, we will only need to consider the equations of motion (2.1) for the $N - 2$ interior particles.

In this system, the initial particle displacements are $u_j(0) = 0$, $j = 1, \dots, N$ (since the chain is initially in its equilibrium configuration). The system is initially uncompressed if $\delta_0 = 0$, in which case the initial separation between adjacent particles is $2R$, where R is the particle radius. Instead, if $\delta_0 > 0$, the system has a pre-compression, in which case the initial separation between adjacent particles is $2R - \delta_0$.

In typical experiments and numerical simulations, the initial particle velocities are $\dot{u}_j(0) = 0$ for the interior particles $j = 2, \dots, N - 1$, while for the two end particles, the velocities $\dot{u}_1(0)$ and $\dot{u}_N(0)$ correspond to imparting an initial impulse at one end or both ends of the chain. An impulse produces a propagating pulse in the system, where the wave amplitude is described by the variable

$$A(t; i) = \delta_0 + u_i(t) - u_{i+1}(t) \geq 0 \quad (2.2)$$

corresponding to the net force on the i^{th} particle, with $A(0; i) = \delta_0$ initially. Experimentally, this variable is measured for one (or a few) particle(s), giving the amplitude $A(t; i)$ as a function of time t at fixed i . For travelling wave pulses, the amplitude profile $A(t; i)$ in t has the same shape as a snapshot of the amplitude $A(t_0; i)$ as a function of particle number i at a fixed time $t = t_0$. The dynamical state of a precompressed system is said to be *weakly compressed* if the dynamical overlap between adjacent moving particles is approximately at least the size of the initial overlap:

$$|\delta_0 + u_i(t) - u_{i+1}(t)| \gtrsim \delta_0 > 0, \quad |\dot{u}_i(t) - \dot{u}_{i+1}(t)| \neq 0, \quad t > 0. \quad (2.3)$$

Note these conditions can be expressed simply as

$$|A(t; i)| \gtrsim \delta_0, \quad \dot{A}(t; i) \neq 0 \quad (2.4)$$

in terms of the amplitude of a pulse.

Experimentally, weakly compressed chains support solitary waves whose observed wavelength [58] is approximately $10R$ in the case of when the contact geometry of the particles is elliptical, which corresponds to $k = 3/2$.

To derive a continuum wave equation for long wavelength pulses in weakly compressed chains, it is useful to begin with a change of variables

$$u_i = U_i + i\delta_0, \quad i = 1, \dots, N \quad (2.5)$$

in the discrete system, so the equations of motion (2.1) become

$$m\ddot{U}_i = (k + 1)a((U_{i-1} - U_i)^k - (U_i - U_{i+1})^k), \quad i = 2, \dots, N - 1. \quad (2.6)$$

Then the continuum limit for this system (2.6) is obtained by replacing

$$U_i(t) \rightarrow U(t, x), \quad U_{i\pm 1}(t) \rightarrow U(t, x \pm 2R) = e^{\pm 2R\partial_x} U(t, x), \quad i = 2, \dots, N - 1 \quad (2.7)$$

with $U_{i-1} - U_i \rightarrow W_-$ and $U_i - U_{i+1} \rightarrow W_+$, where

$$\pm W_{\pm} = U(t, x) - U(t, x \pm 2R) = U - e^{\pm 2R\partial_x} U = - \sum_{n=1}^{\infty} \frac{(\pm 2R)^n}{n!} \partial_x^n U. \quad (2.8)$$

This yields

$$\frac{m}{a(k+1)} U_{tt} = W_-^k - W_+^k \quad (2.9)$$

which is a continuum wave equation for $U(t, x)$. The continuum limit of the wave amplitude $A(t; i)$ from the discrete system is given by $A(t; i) = \delta_0 + u_i - u_{i+1} = U_i - U_{i+1} \rightarrow W_+$ which is a nonlocal variable. What is measured experimentally, however, corresponds to the local part of $W_+ = -2RU_x \left(1 + \sum_{n=1}^{\infty} \frac{(2R)^n}{(n+1)!} (\partial_x^{n+1} U) / U_x \right)$ as given by the leading term $-2RU_x$. Up to the factor $2R$, this local variable physically represents the (dimensionless) strain

$$v = -U_x \quad (2.10)$$

while $U(t, x)$ then represents the displacement for the continuum system. The conditions (2.2) and (2.4) on $A(t; i)$ imply that the strain must satisfy the corresponding conditions

$$v > 0, \quad |v| \gtrsim \frac{\delta_0}{2R}. \quad (2.11)$$

Since there is non-zero pre-compression, note $A(0; i) = \delta_0 \rightarrow W_+|_{t=0}$ and, consequently, the initial strain is given by

$$v|_{t=0} = v_0 = \frac{\delta_0}{2R} > 0. \quad (2.12)$$

The next step consists of making a long wavelength expansion of the continuum wave equation (2.9) for $U(t, x)$. Consider a pulse of wavelength ℓ , where $v = O(1)$ and $v_x = O(1/\ell)$ in terms of the strain. The condition for the wavelength to be long is $\ell \gg 2R$. This can be expressed by the parameter $\epsilon = 2R/\ell \ll 1$. The nonlinear terms in the wave equation (2.9) can be expanded in terms of ϵ through the relation $(2R)^n \partial_x^n v = O(\epsilon^n)$, using

$$W_{\pm}^k = (2R)^k \left(v + \sum_{n=1}^{\infty} \frac{(\pm 2R)^n}{(n+1)!} \partial_x^n v \right)^k \quad (2.13)$$

where v is $O(1)$. This gives

$$\begin{aligned} W_{\pm}^k &= (2R)^k \left(v^k \pm kRv^{k-1}v_x + \frac{2}{3}kR^2v^{k-1}v_{xx} + \frac{1}{2}k(k-1)R^2v^{k-2}v_x^2 \right. \\ &\quad \left. \pm \frac{1}{3}kR^3v^{k-1}v_{xxx} \pm \frac{2}{3}k(k-1)R^3v^{k-2}v_xv_{xx} \pm \frac{1}{6}k(k-1)(k-2)R^3v^{k-3}v_x^3 \right. \\ &\quad \left. + \frac{1}{18}k(k-1)R^4v^{k-2}(4v_{xx}^2 + 3v_xv_{xxx}) + \dots \right) \end{aligned} \quad (2.14)$$

up to order $O(\epsilon^4)$, which yields

$$\begin{aligned} \frac{m}{a(k+1)}U_{tt} = W_-^k - W_+^k &= \left((-U_x)^{k-1}U_{xx} + \frac{1}{6}R^2((k-1)(k-2)(-U_x)^{k-3}U_{xx}^3 \right. \\ &\quad \left. - 4(k-1)(-U_x)^{k-2}U_{xx}U_{xxx} + 2(-U_x)^{k-1}U_{xxxx}) + \dots \right). \end{aligned} \quad (2.15)$$

Truncating the expansion at this order $O(\epsilon^4)$ and substituting the strain expression (2.10) produces the well-known highly nonlinear fourth-order wave equation [3, 18, 29, 32] for $U(t, x)$:

$$c^{-2}U_{tt} = (-U_x)^{k-1}U_{xx} + \alpha(-U_x)^{k-3}U_{xx}^3 - \beta(-U_x)^{k-2}U_{xx}U_{xxx} + \gamma(-U_x)^{k-1}U_{xxxx} \quad (2.16)$$

where

$$\alpha = \frac{1}{6}R^2(k-1)(k-2), \quad \beta = \frac{2}{3}R^2(k-1), \quad \gamma = \frac{1}{3}R^2 \quad (2.17)$$

and

$$c^2 = ak(k+1)(2R)^{k+1}/m. \quad (2.18)$$

Note, in these expressions (2.17)–(2.18), the constant c has units of speed, and the constants α , β , γ have units of length-squared, while U has units of length. We will call equation (2.16) the *long-wavelength Hertzian continuum* (LWHC) wave equation.

There is a corresponding long-wavelength wave equation for the strain $v(t, x)$:

$$c^{-2}v_{tt} = (v^{k-1}v_x + \alpha v^{k-3}v_x^3 + \beta v^{k-2}v_xv_{xx} + \gamma v^{k-1}v_{xxx})_x \quad (2.19)$$

with v satisfying the conditions (2.11) and (2.12).

2.1. Linearized (sound) waves. In the continuum limit, waves that have very small amplitude relative to the size of the pre-compression physically describe the linearized sound waves of the continuum system. Long wavelength sound waves are given by $V = v - v_0$ where $0 < V \ll v_0 = \delta_0/(2R)$ satisfies the linearization of the long-wavelength wave equation (2.19). This linearized wave equation has the form

$$c^{-2}V_{tt} = (v_0^{k-1}V_x + \gamma v_0^{k-1}V_{xxx})_x \quad (2.20)$$

where $\gamma = \frac{1}{3}R^2$. To obtain the dispersion relation, we substitute a harmonic mode expression $V = e^{i(\kappa x - \omega t)}$ into this wave equation, yielding $c^{-2}\omega^2 = v_0^{k-1}\kappa^2 - \frac{1}{3}R^2v_0^{k-1}\kappa^4$. Since the wavelength is $\ell = 2\pi/\kappa$, which obeys $2R/\ell \ll 1$, we see that $c^{-2}\omega^2 = v_0^{k-1}(2\pi/\ell)^2(1 - \frac{\pi^2}{3}(2R/\ell)^2)$ can be approximated by $c^{-2}\omega^2 \simeq v_0^{k-1}(2\pi/\ell)^2$. This yields a linear dispersion relation

$$\pm \omega \simeq v_0^{(k-1)/2} c \kappa. \quad (2.21)$$

Hence the sound speed is given by

$$c_0 = \omega/\kappa = \left(\frac{\delta_0}{2R}\right)^{(k-1)/2} c. \quad (2.22)$$

2.2. Conservation laws. A conservation law for the LWHC wave equation (2.16) is a local continuity equation

$$D_t T + D_x X = 0 \quad (2.23)$$

holding for all solutions $U(t, x)$ of the wave equation, where T is the conserved density and X is the spatial flux, which are given by functions of t, x, U, U_t , and x -derivatives of U and U_t . As shown in Ref. [62], all conservation laws with conserved densities of the first-order form $T(t, x, U, U_t, U_x)$ are given by:

$$T_1 = -U_t U_x, \quad (2.24)$$

$$X_1 = \frac{1}{2}U_t^2 - c^2\left(\frac{1}{3}R^2(-U_x)^k U_{xxx} - \frac{k-2}{6}R^2(-U_x)^{k-1}U_{xx}^2 - \frac{1}{k+1}(-U_x)^{k+1}\right);$$

$$T_2 = \frac{1}{2}U_t^2 - c^2\left(\frac{1}{6}R^2(-U_x)^{k-1}U_{xx}^2 - \frac{1}{k(k+1)}(-U_x)^{k+1}\right), \quad (2.25)$$

$$X_2 = -c^2\left(\frac{1}{3}R^2(-U_x)^{k-1}(U_t U_{xxx} - U_{tx} U_{xx}) - \frac{k-1}{6}R^2(-U_x)^{k-2}U_t U_{xx}^2 - \frac{1}{k}(-U_x)^k U_t\right);$$

$$T_3 = U_t, \quad (2.26)$$

$$X_3 = c^2\left(-\frac{1}{3}R^2(-U_x)^{k-1}U_{xxx} + \frac{k-1}{6}R^2(-U_x)^{k-2}U_{xx}^2 + \frac{1}{k}(-U_x)^k\right);$$

$$T_4 = U - tU_t, \quad (2.27)$$

$$X_4 = c^2 t \left(\frac{1}{3}R^2(-U_x)^{k-1}U_{xxx} - \frac{k-1}{6}R^2(-U_x)^{k-2}U_{xx}^2 - \frac{1}{k}(-U_x)^k\right).$$

Conservation laws (2.24) and (2.25) respectively describe the total energy and momentum of solutions $U(t, x)$. Conservation law (2.26) describes the total impulse, while conservation law (2.27) is connected with the mean value of $U(t, x)$.

3. SINGLE-ARCH TRAVELLING WAVE (COMPACTON) AND EXACT SOLITARY WAVES

We are interested in travelling wave solutions

$$U = f(\zeta), \quad \zeta = x - \nu t \quad (3.1)$$

of the LWHC wave equation (2.16). Substitution of this ansatz (3.1) into equation (2.16) yields a fourth-order differential equation

$$(\nu/c)^2 f'' = (-f')^{k-1} f'' + \alpha(-f')^{k-3} (f'')^3 - \beta(f')^{k-2} f'' f''' + \gamma(-f')^{k-1} f'''' \quad (3.2)$$

where ν is the (constant) wave velocity, and where c , α , β , γ are given by expressions (2.17)–(2.18).

The physical variable that will support solitary waves is the strain (2.10). For a travelling wave (3.1), this variable has the form

$$v = -f'(\zeta) > 0. \quad (3.3)$$

Since a solitary wave has a localized profile in ζ , we want solutions for which $-f'(\zeta)$ is a localized expression in ζ and has an asymptotic value given by the initial value (2.12) for the strain,

$$\lim_{\zeta \rightarrow \pm\infty} (-f'(\zeta)) = \frac{\delta_0}{2R} > 0. \quad (3.4)$$

It will be useful, mathematically, to work with dimensionless scaled variables:

$$g = -f'/\lambda, \quad \xi = \zeta/l \quad (3.5)$$

with

$$\lambda = \left(\frac{1}{2}(\nu/c)^2 k(k+1)\right)^{1/(k-1)}, \quad l = \sqrt{\frac{1}{6}k(k+1)}R. \quad (3.6)$$

The inverse transformation from $g(\xi)$ to $v(t, x)$ is given by

$$v(t, x) = \lambda g((x - \nu t)/l). \quad (3.7)$$

In terms of these scaled variables (3.5), the travelling wave equation (3.2) becomes a third-order differential equation for $g(\xi)$

$$0 = 2g^{k-1}g''' + 4(k-1)g^{k-2}g'g'' + (k-1)(k-2)g^{k-3}g'^3 + k(k+1)g^{k-1}g' - 2g', \quad (3.8)$$

and the asymptotic condition (3.4) on solutions becomes

$$\lim_{\xi \rightarrow \pm\infty} g(\xi) = g_0 > 0 \quad (3.9)$$

where

$$g_0 = \frac{\delta_0}{2R} \left(\frac{1}{2}(\nu/c)^2 k(k+1)\right)^{1/(1-k)}. \quad (3.10)$$

This third-order differential equation (3.8) can be directly reduced to a first-order separable differential equation by using first integrals that arise from the conservation laws (2.24)–(2.26) (which do not contain t and x explicitly) admitted by the LWHC wave equation (2.16), as explained in Ref. [62]. This yields

$$(g')^2 = g^{1-k}(g^2 + C_1 g + C_2 - g^{1+k}) \quad (3.11)$$

where C_1 and C_2 are dimensionless arbitrary constants which correspond to scaled first integrals. The physical meaning of the two first integrals are, respectively, the spatial flux of the impulse in the rest frame of the travelling wave, and the spatial flux of energy/momentum in the rest frame of the travelling wave. Thus, for any solution $g(\xi)$, $C_2 = E$ represents a dimensionless energy and $C_1 = I$ represents a dimensionless impulse.

We now view the first-order differential equation (3.11) as being analogous to the energy integral for motion in a potential well

$$g^{k-1}g'^2 + V(g) = E \quad (3.12)$$

where $g^{k-1}g'^2$ plays the role of the kinetic energy, and where the potential energy is given by

$$V(g) = g^{1+k} - g(g + I) \quad (3.13)$$

which depends on a free parameter I . A comprehensive qualitative analysis has been carried out in Ref. [62] to determine the values of (E, I) that lead to solitary wave solutions for $g(\xi)$ with the asymptotic boundary condition (3.9). This depends crucially on the shape of the potential (3.13). We next summarize this analysis.

3.1. Exact solitary waves. Solitary waves exist when (and only when) $V(g) = E$ has two roots $g = g_0$ and $g = g_1$ such that $V'(g_0) = 0$ and $V'(g_1) > 0$ with

$$0 < g_0 < g^* < g_1 < 1 \quad (3.14)$$

where

$$g^* = \left(\frac{2}{k(k+1)}\right)^{1/(k-1)} \quad (3.15)$$

is the point at which $V''(g) = 0$. The relationship between g_0 and (E, I) is given by

$$E = g_0^2(1 - kg_0^{k-1}), \quad I = (k+1)g_0^k - 2g_0 \quad (3.16)$$

which leads to the corresponding parameter ranges

$$E > 0, \quad 0 > I > I^* \quad (3.17)$$

where

$$I^* = (1+k)g^{*k} - 2g^* = -\frac{2(k-1)}{k}g^* < 0. \quad (3.18)$$

Note

$$0 < g^* < 1 \quad (3.19)$$

since $k > 1$. Also note g_1 is a function of g_0 as given by the root of the algebraic equation

$$0 = V(g_1) - E = g_1^{k+1} - g_1^2 + g_0(2 - (k+1)g_0^{k-1})g_1 + g_0^2(kg_0^{k-1} - 1) \quad (3.20)$$

where $0 < g_0 < g^*$. As shown in [62], g_1 is a decreasing function of g_0 , with $g_1 \rightarrow 1$ when $g_0 \rightarrow 0$, and $g_1 \rightarrow g^*$ when $g_0 \rightarrow g^*$.

All solitary wave solutions are then given by the integral

$$\pm \int_{g_0}^{g_1} \frac{g^{(k-1)/2}}{\sqrt{E - V(g)}} dg = \xi \quad (3.21)$$

which determines $g(\xi)$. These solutions have a peak amplitude $g = g_1$ at $\xi = 0$, and an asymptotic tail with exponential decay $g \rightarrow g_0$ as $|\xi| \rightarrow \infty$, where g_1 is determined by the algebraic equation (3.20) in terms of g_0 , and where g_0 obeys the inequality (3.14). Interestingly, this inequality can be expressed as a corresponding relation between the solitary wave speed ν and the sound speed (2.22), as follows. First, we note that the expression (3.10) for g_0 can be written as $g_0/g^* = \frac{\delta_0}{2R}(c/|\nu|)^{2/(k-1)}$. Next, we can write $\frac{\delta_0}{2R} = (c_0/c)^{2/(k-1)}$ from the expression (2.22) for the sound speed c_0 . Combining these two expressions yields $g_0/g^* = (c_0/|\nu|)^{2/(k-1)}$, and hence the inequality (3.14) is equivalent to

$$|\nu| > c_0. \quad (3.22)$$

This shows that all solitary waves are supersonic, which is a well-known statement in the literature.

We showed in Ref. [62] that the quadrature (3.21) can be evaluated in terms of elementary functions when $k = 2, 3$, and in terms of elliptic functions when $k = \frac{3}{2}, 4, 5$. All of these cases lead to implicit algebraic expressions for $g(\xi)$.

For the cases $k = 2$ and $k = 3$, the respective solutions are given by

$$\frac{g_0}{\sqrt{P(g_0)}} \operatorname{arctanh}(Q(g)) + \arctan\left(\frac{\sqrt{P(g)}}{g + g_0 - \frac{1}{2}}\right) = \pm\xi, \quad (3.23)$$

with

$$P(g) = (g_1 - g)g, \quad g_1 = 1 - 2g_0, \quad g^* = 1/3, \quad (3.24)$$

and

$$\frac{g_0}{\sqrt{P(g_0)}} \operatorname{arctanh}(Q(g)) + \arctan\left(\frac{\sqrt{P(g)}}{g + g_0}\right) = \pm\xi, \quad (3.25)$$

with

$$P(g) = (g_1 - g)(g + g_1 + 2g_0), \quad g_1 = \sqrt{1 - 2g_0^2} - g_0, \quad g^* = 1/\sqrt{6}, \quad (3.26)$$

where

$$Q(g) = \frac{2\sqrt{P(g)P(g_0)}}{P(g) + P(g_0) + (g - g_0)^2}. \quad (3.27)$$

In both cases, g_0 is a free parameter in the range $0 < g_0 < g^*$, and g_1 is given explicitly in terms of g_0 . (Note, here \arctan is defined to be continuous in the given range for g_0 .) See Fig. 1(b,c).

For the case $k = \frac{3}{2}$, the solution is given by

$$I(\sqrt{g}) + J(\sqrt{g}) = \pm\xi, \quad g = h^2 \quad (3.28)$$

where

$$I(h) = \sigma \ln \left(\frac{2\sqrt{\Gamma}(Y(h)/Y_0 + \sqrt{X(h)/X_0})(\sqrt{X(h)} + \sqrt{X_0})((h + h_2)^2 + h_3^2)}{\Lambda(h - h_0)(1 + Y(h)/Y_0)\sqrt{1 + \varpi X(h)}} \right) + \arctan \left(\frac{2\sqrt{X(h)}}{1 - X(h)} \right) \quad (3.29)$$

is a sum of elementary functions given in terms of the rational functions

$$X(h) = \frac{h(h_1 - h)}{(h + h_2)^2 + h_3^2}, \quad Y(h) = \frac{h - h_1/\Phi_+}{h + h_1/\Phi_-} \quad (3.30)$$

and where

$$J(h) = \eta((\theta - \phi)Z(h) + \Pi(-\mu; Z(h)|\psi) - \theta\Pi(\nu; Z(h)|\psi)) \quad (3.31)$$

is a sum of Jacobi elliptic functions (of the third kind) [64]

$$\Pi(n; \theta|l) = \frac{1}{\sqrt{1+j}} \int_{\operatorname{cn}(\theta|l)}^1 \frac{dz}{(mz^2 - 1)\sqrt{(1 - z^2)(1 + jz^2)}}, \quad (3.32)$$

$$l = j/(j + 1), \quad n = m/(m - 1), \quad j > 0,$$

with

$$Z(h) = \operatorname{cn}^{-1}((\Phi_+/\Phi_-)Y(h)|\psi) \quad (3.33)$$

being given by the inverse of the cn elliptic function. The constants in expressions (3.29) – (3.33) are given by

$$X_0 = X(h_0), \quad Y_0 = Y(h_0), \quad W_0 = (h_0 + h_2)^2 + h_3^2, \quad W_1 = (h_1 + h_2)^2 + h_3^2, \quad (3.34)$$

$$\sigma = \frac{2h_0^2}{\sqrt{h_0(h_1 - h_0)W_0}}, \quad \varpi = \frac{Y_0^2 \Phi_+^2}{\Phi_-^2} (1 - 1/\Omega^2), \quad (3.35)$$

$$\eta = \frac{2\Omega\Phi_+}{\Phi_- \sqrt{2(\Phi_+ + \Phi_-)}}, \quad \phi = (1 - Y_0)\Lambda, \quad \theta = \frac{h_0 Y_0}{h_1 - h_0}, \quad (3.36)$$

$$\psi = (\Omega^2 - 1) \frac{\Phi_-^2}{2(\Phi_+ + \Phi_-)}, \quad \mu = \frac{\psi}{\Omega^2 - 1}, \quad \nu = \frac{\psi\Gamma}{2(\Phi_+ + \Phi_-)}, \quad (3.37)$$

$$\Phi_{\pm} = \frac{\sqrt{W_1}}{\sqrt{h_2^2 + h_3^2}} \pm 1, \quad \Omega = \frac{h_1}{\Phi_- \sqrt{h_2^2 + h_3^2}}, \quad \Gamma = \frac{h_0(h_1 - h_0)}{(\Phi_- h_0 + h_1)^2}, \quad \Lambda = \frac{\sqrt{h_2^2 + h_3^2}}{\sqrt{W_0}}, \quad (3.38)$$

with

$$h_1 = \frac{1}{3} - \frac{2}{3}h_0 + r_-^{1/3} - r_+^{1/3}, \quad (3.39)$$

$$h_2 = -\frac{1}{3} + \frac{2}{3}h_0 + \frac{1}{2}(r_-^{1/3} - r_+^{1/3}), \quad (3.40)$$

$$h_2^2 + h_3^2 = (h_0 - \frac{2}{3})h_0 + r_-^{2/3} + r_+^{2/3} + (\frac{2}{3}h_0 - \frac{1}{3})(r_-^{1/3} - r_+^{1/3}), \quad (3.41)$$

$$r_{\pm} = \frac{5}{12} \sqrt{h_0^3(h_0 - \frac{2}{3})(h_0^2 - \frac{2}{5}h_0 - \frac{4}{25})} \pm \frac{5}{108}(h_0^3 + \frac{24}{5}h_0^2 - \frac{12}{5}h_0 - \frac{4}{5}). \quad (3.42)$$

In this solution, all of these constants depend only on h_0 which is a free parameter in the range $0 < h_0 < h^* = \frac{8}{15}$, corresponding to $0 < g_0 < g^* = \frac{64}{225}$. Furthermore, the constants (3.34)–(3.38) are positive. (Some details of the derivation of the solution are shown in the Appendix.) See Fig. 1(a).

The solutions for the other two cases $k = 4$ and $k = 5$ are similar to the case $k = \frac{3}{2}$ and will be omitted.

3.2. Single-arch travelling wave (compacton). A compacton exists when $V(g) = E$ has two roots $g = 0$ and $g = 1 > g^*$ such that $V'(0) = 0$ and $V'(1) > 0$. This implies

$$E = I = 0 \quad (3.43)$$

which are the limiting values of E and I in the case of solitary waves when the parameter g_0 goes to 0. We note that the potential (3.13) with $I = 0$ no longer has a local maximum for $g > 0$.

For the values (3.43), the solution $g(\xi)$ of the ODE (3.12) is given by the integral

$$\pm \int_g^1 \frac{g^{(k-3)/2}}{\sqrt{1 - g^{k-1}}} dg = \xi. \quad (3.44)$$

This integral can be seen to coincide with the limit $g_0 \rightarrow 0$ of the integral (3.21) for solitary waves, since in this limit we have $E \rightarrow 0$ and $I \rightarrow 0$ whereby $E - V(g) \rightarrow g^2 - g^{1+k}$ which yields $g_1 \rightarrow 1$.

This integral (3.44) can be evaluated explicitly, yielding

$$g(\xi) = \cos\left(\frac{1}{2}(k-1)|\xi - L[\frac{1}{2} + \xi/L]|\right)^{2/(k-1)} \geq 0, \quad L = \frac{2\pi}{k-1} \quad (3.45)$$

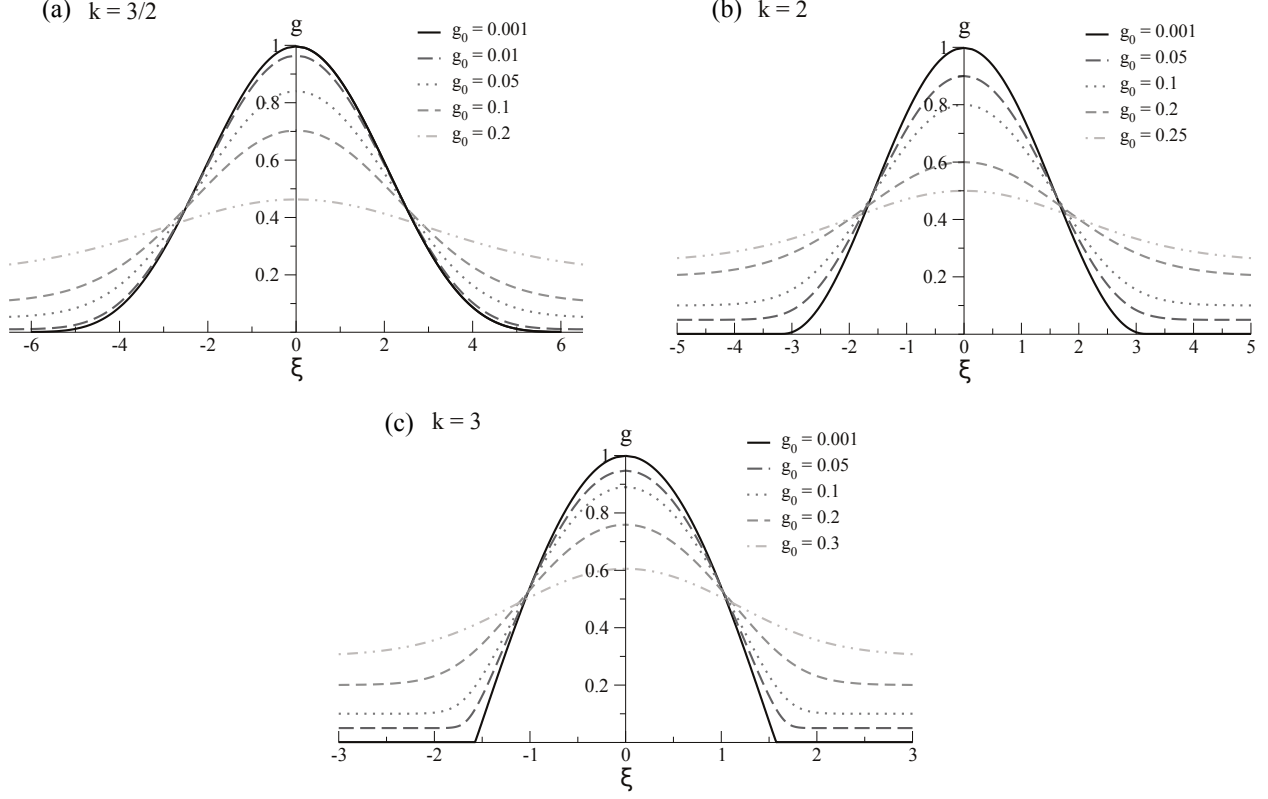


FIGURE 1. Solitary wave solutions for $k = \frac{3}{2}, 2, 3$

where $\lfloor x \rfloor$ denotes the floor function. The solution is a periodic function of ξ having a peak amplitude $g = 1$ at $\xi = 0 \pmod L$, and a node $g = 0$ at $\xi = \pm L/2 \pmod L$. The node is a minimum if $1 < k < 3$, or a corner if $k = 3$, or a cusp if $k > 3$. We remark that this solution (3.45) has appeared in Ref. [18, 32] but with the phase shift omitted. Without the phase shift, the power $2/(k-1)$ must be interpreted as the $(k-1)^{\text{th}}$ positive real root of the square of the cosine.

Since the periodic solution (3.45) has a node at $\xi = \pm L/2$, we can cut off this solution expression at these two points and take $g(\xi)$ to vanish outside the domain $-L/2 \leq \xi \leq L/2$. This yields a piecewise expression

$$g(\xi) = \begin{cases} \cos\left(\frac{1}{2}(k-1)\xi\right)^{2/(k-1)}, & |\xi| \leq \pi/(k-1) \\ 0, & |\xi| \geq \pi/(k-1) \end{cases} \quad (3.46)$$

which is continuous at the nodal points $\xi = \pm L/2$. However, this piecewise expression needs to be three-times differentiable for it to be an actual solution of the travelling wave ODE (3.8). In particular, we must have $0 = g_{\text{per.}}(\pm L/2) = g'_{\text{per.}}(\pm L/2) = g''_{\text{per.}}(\pm L/2) = g'''_{\text{per.}}(\pm L/2)$, where $g_{\text{per.}}(\xi)$ denotes the periodic solution (3.45). These conditions are easily verified to hold if and only if $1 < k < 5/3$.

The resulting solution (3.46), which consists of a single arch of the periodic solution (3.45), is a compacton. It exists only for k in the range

$$1 < k < 5/3. \quad (3.47)$$

This condition on k is often overlooked in the literature.

4. COMPARISON OF PROPERTIES

Our goal is to compare the physical properties of the solitary wave solutions and the compacton solution of the long-wavelength Hertzian continuum (LWHC) wave equation (2.16).

In experiments on pre-compressed chains, pulses are generated by striking an end particle in the chain. This corresponds to imparting a specified total impulse to the discrete system. For the continuum system, described by the LWHC wave equation, the total impulse is given by a conserved integral

$$\tilde{\mathcal{I}} = \int_{-\infty}^{\infty} U_t dx \quad (4.1)$$

arising from the the impulse conservation law (2.26) for solutions $U(t, x)$. In the case when $U(t, x)$ is a travelling wave solution (3.1), the conserved impulse integral has the form

$$\tilde{\mathcal{I}} = \frac{1}{\sqrt{3}}(1/g^*)^{(k+1)/2} Rc^{2/(1-k)} \text{sgn}(\nu) |\nu|^{(k+1)/(k-1)} \int_{-\infty}^{\infty} g(\xi) d\xi \quad (4.2)$$

where $g(\xi)$ is a scaled strain variable (3.5)–(3.6) satisfying the differential equation (3.12) for motion in a potential well (3.13). Note g^* is expression (3.15) given in terms of k .

The impulse integral (4.2) is finite for the compacton solution (3.46), since $g(\xi)$ vanishes outside of the finite interval $0 \leq |\xi| \leq \frac{\pi}{k-1}$. In contrast, solitary wave solutions (3.21) have a non-zero asymptotic value $g(\xi) \rightarrow g_0 > 0$ as $\xi \rightarrow \pm\infty$, and hence the impulse integral (4.2) will be infinite. However, we can regularize it to remove the divergent contribution by subtracting the impulse density given by the constant solution $g = g_0$ of the differential equation (3.12), where E has the value (3.16) appropriate for solitary waves. This gives the regularized impulse integral

$$\mathcal{I} = \frac{1}{\sqrt{3}}(1/g^*)^{(k+1)/2} Rc^{2/(1-k)} \text{sgn}(\nu) |\nu|^{(k+1)/(k-1)} \int_{-\infty}^{\infty} (g(\xi) - g_0) d\xi \quad (4.3)$$

which will be finite for all solitary wave solutions. Moreover, since the compacton solution corresponds to the $g_0 \rightarrow 0$ limit of the solitary wave solutions, the regularized impulse integral (4.3) applies as well to the compacton solution.

We note that this impulse integral displays the scaling relation $I \propto |\nu|^{(k+1)/(k-1)}$ in terms of the speed ν of the travelling wave. In particular, for a fixed value of the impulse, the speed scales like $|\nu| \propto \mathcal{I}^{(k-1)/(k+1)}$, where $k+1$ is the exponent in the contact potential. This scaling relation has the same form as the one given in the literature [30] for pre-compressed discrete chains (2.1).

To evaluate the impulse integral \mathcal{I} for the solitary wave solutions and the compacton solution, we will use the method from Ref. [62] to convert the integration variable from ξ to g by using the differential equation (3.12). This change of variable relies on the global features that $g(\xi)$ is a symmetric function of ξ having a single maximum amplitude g_1 at $\xi = 0$ and a minimum amplitude g_0 at $\xi \rightarrow \pm\infty$. Hence, we obtain

$$\mathcal{I} = \frac{2}{\sqrt{3}}(1/g^*)^{(k+1)/2} Rc^{2/(1-k)} \text{sgn}(\nu) |\nu|^{(k+1)/(k-1)} \mathcal{C}(g_0) \quad (4.4)$$

where

$$\mathcal{C}(g_0) = \int_{g_0}^{g_1} \frac{g^{(k-1)/2}(g - g_0)}{\sqrt{E - V(g)}} dg. \quad (4.5)$$

We will now proceed to examine the physical properties of the solitary wave solutions (3.21) and the compacton solution (3.46), with a fixed value of the impulse integral (4.4).

4.1. Physical properties of solitary waves. In physical variables (3.7), all solitary waves $v(x - \nu t)$ are given by

$$\pm \int_{(c/|\nu|)^{2/(k-1)}g^*v}^{(c/|\nu|)^{2/(k-1)}g^*v_1} \frac{g^{(k-1)/2}}{\sqrt{E - V(g)}} dg = \sqrt{3}g^{*k-1}(x - \nu t)/R \quad (4.6)$$

where g^* is expression (3.15) given in terms of k , and where

$$v_1 = (|\nu|/c)^{2/(k-1)}g_1/g^* \quad (4.7)$$

is the peak strain in the wave.

The impulse integral (4.4) for solitary waves involves two free parameters: ν , which is the wave speed, and g_0 , which is the scaled value of the asymptotic strain (2.12) as given by the relation

$$v_0 = (|\nu|/c)^{2/(k-1)}g_0/g^*. \quad (4.8)$$

By expressing g_0 in terms of ν and v_0 , we can equivalently regard the impulse integral as being a function of the physical parameters ν and v_0 :

$$\mathcal{I}_s(\nu, v_0) = \frac{2}{\sqrt{3}}(1/g^*)^{(k+1)/2} R c^{2/(1-k)} \text{sgn}(\nu) |\nu|^{(k+1)/(k-1)} \mathcal{C}((c/|\nu|)^{2/(k-1)}v_0g^*). \quad (4.9)$$

Note the speed ν can be arbitrary, while the asymptotic strain v_0 is constrained by the inequality (3.14). This implies

$$0 \leq |\nu| < \infty, \quad 0 < v_0 < v^*, \quad v^* = (|\nu|/c)^{2/(k-1)} \quad (4.10)$$

or, equivalently,

$$|\nu| > v_0^{(k-1)/2}c > 0. \quad (4.11)$$

If we fix the wave speed $\nu \neq 0$, then the asymptotic strain v_0 has the range (4.10). At the end points of this range, the value of the expression $\mathcal{C}((c/|\nu|)^{2/(k-1)}v_0g^*)$ is given by

$$\mathcal{C}(0) = \sqrt{\pi}\Gamma\left(\frac{k+1}{2k-2}\right)/\Gamma\left(\frac{1}{k-1}\right), \quad \mathcal{C}(g^*) = 0. \quad (4.12)$$

In the interior of the range (4.10) for v_0 , a numerical investigation of the expression $\mathcal{C}((c/|\nu|)^{2/(k-1)}v_0g^*)$ indicates that it is a decreasing function of v_0 and that its derivative becomes large as $v_0 \rightarrow v^*$. Consequently, we can approximate this function by taking

$$\mathcal{C}(g_0) \approx \tilde{\mathcal{C}}(g_0) = a(g^* - g_0) + b\sqrt{g^* - g_0} \quad (4.13)$$

where $a = \frac{2\pi}{k-1} - \mathcal{C}(0)\frac{1}{g^*}$ and $b = \frac{2}{\sqrt{g^*}}\mathcal{C}(0) - \frac{2\pi\sqrt{g^*}}{k-1}$ are constants determined so that $\tilde{\mathcal{C}}(0) = \mathcal{C}(0)$ and $\tilde{\mathcal{C}}'(0) = \mathcal{C}'(0)$ match at $g_0 = 0$, while $\tilde{\mathcal{C}}(g^*) = 0$. We find $\mathcal{C}'(0) = \frac{\pi}{1-k}$ from the integral expression (4.5) combined with equation (3.20) for $g_1(g_0)$.

Hence, we conclude that the impulse integral (4.9) has a maximum when the strain vanishes, and decreases to a minimum of zero when strain has the value $v_0 = (|\nu|/c)^{2/(k-1)}$. In particular,

$$\mathcal{I}_{s,\max} = \mathcal{I}_s(\nu, 0) = K R c^{2/(1-k)} \text{sgn}(\nu) |\nu|^{(k+1)/(k-1)}, \quad \mathcal{I}_{s,\min} = \mathcal{I}_s(\nu, (|\nu|/c)^{2/(k-1)}) = 0 \quad (4.14)$$

where $K = \frac{2\sqrt{\pi}}{\sqrt{3}}(1/g^*)^{(k+1)/2}\Gamma(\frac{k+1}{2k-2})/\Gamma(\frac{1}{k-1})$ is a constant depending only on k . A useful approximate formula for the impulse integral is given by

$$\mathcal{I}_s(\nu, v_0) \approx KRc^{2/(1-k)}\text{sgn}(\nu)|\nu|^{(k+1)/(k-1)}\left((\tilde{K}-1)(1-v_0/v^*)+(2-\tilde{K})\sqrt{1-v_0/v^*}\right) \quad (4.15)$$

where

$$\tilde{K} = 2\sqrt{\pi}g^*\Gamma(\frac{k}{k-1})/\Gamma(\frac{k+1}{2k-2}). \quad (4.16)$$

We now consider fixing the value of the impulse integral (4.9). Then there is a one-parameter family of solitary wave solutions, where either ν or v_0 is the free parameter subject to the inequalities (4.10), or equivalently, (4.11). This shows that, physically, a unique solitary wave is not determined by specifying only the impulse imparted to a pre-compressed continuum system.

To understand all of the distinct solitary waves that have the same value of the impulse (4.9), we focus on their height and width.

The physical height, h_s , of a solitary wave is measured by the peak amplitude of the strain v relative to the asymptotic strain v_0 ,

$$h_s = v_1 - v_0 \quad (4.17)$$

where v_1 is the maximum strain in the wave. For fixed wave speed ν , note v_0 determines g_0 through the relation (4.8), which in turn determines g_1 by the algebraic equation (3.20), giving v_1 as a function of v_0 , whereby

$$h_s = (|\nu|/c)^{2/(k-1)}g_1(v_0g^*(c/|\nu|)^{2/(k-1)})/g^* - v_0 = H_s(v_0; \nu). \quad (4.18)$$

This height function has the following main features. From the properties of $g_1(g_0)$ shown in Ref. [62], we have that $H(v_0; \nu)$ is a decreasing function of v_0 , with v_0 given by the range (4.10), and that $H(v_0; \nu)$ has the limiting values

$$h_{s,\max} = H_s(0; \nu) = (|\nu|/c)^{2/(k-1)}/g^*, \quad h_{s,\min} = H_s(v^*; \nu) = 0 \quad (4.19)$$

at the end points $v_0 \rightarrow 0$ and $v_0 \rightarrow v^*$ of the range.

The physical width, ℓ_s , of a solitary wave can be measured by finding the position $|\zeta|$ at which the relative height of the wave is a fraction $0 < \varepsilon < 1$ of the peak amplitude of the strain $v(\zeta)$ relative to the asymptotic strain v_0 :

$$v(|\zeta|) = v_0 + \varepsilon h. \quad (4.20)$$

This condition can be converted into the convenient form

$$|\zeta| = |\xi|\sqrt{\frac{k(k+1)}{6}}R, \quad g(|\xi|) = g_0 + \varepsilon(g_1 - g_0) \quad (4.21)$$

in terms of $g(\xi)$, using the transformation (3.7). We substitute the condition (4.21) into the formula (3.21) for the solitary wave solutions, which yields the physical width $\ell_s = 2|\zeta|$ since the wave profile is symmetric about $\zeta = 0$. Therefore, an exact integral formula for the physical width of a solitary wave is given by

$$\ell_s/(2R) = \sqrt{\frac{k(k+1)}{6}} \int_{(1-\varepsilon)g_0 + \varepsilon g_1(g_0)}^{g_1(g_0)} \frac{g^{(k-1)/2}}{\sqrt{E - V(g)}} dg \quad (4.22)$$

with $g_0 = g^*(c/|\nu|)^{2/(k-1)}v_0$. Note this formula (4.22) gives the physical width as a function of the fraction $0 < \varepsilon < 1$, which we are free to choose. A choice of the parameter ε giving

the full width at half-maximum is $\varepsilon = \frac{1}{2}$. But for a later comparison with the width of the compacton solution, we want to take $\varepsilon \lesssim \frac{1}{100}$.

The width formula (4.22) will yield $\ell_s \rightarrow \infty$ as $\varepsilon \rightarrow 0$. It would be natural to expand this formula asymptotically in terms of $\varepsilon \rightarrow 0$ and retain just the leading term. However, standard asymptotic methods [65] will not directly work on this formula because the integrand is singular at the end point $g = g_1$, due to $E - V(g_1) = 0$. Instead we can get a useful approximation by the following steps. We begin by using a change of variable $z = (g - g_0)/(g_1 - g_0)$ combined with the results $E - V(g) = (g - g_0)^2 A(g)$ and $A(g) = (g_1 - g)B(g)$, where $B(g)$ is a non-singular, positive function for $g_0 \leq g \leq g_1$, as derived in Ref. [62]. This gives

$$\int_{g_0 + \varepsilon(g_1 - g_0)}^{g_1} \frac{g^{(k-1)/2}}{\sqrt{E - V(g)}} dg = \int_{\varepsilon}^1 \frac{C(g_0 + z(g_1 - g_0))}{z\sqrt{1-z}} dz \quad (4.23)$$

where $C(g) = g^{(k-1)/2}/\sqrt{(g_1 - g)B(g)}$ is a non-singular, positive function of g . We next approximate $C(g)$ by Simpson's rule $C(g_0 + z(g_1 - g_0)) \approx \tilde{C}(z) = a(z-1)^2 + b(z-1) + c$ such that $\tilde{C}(1) = C(g_1) = c$, $\tilde{C}(z^*) = C(g^*) = a(z^*-1)^2 + b(z^*-1) + c$, $\tilde{C}(\varepsilon) = C(g_0 + \varepsilon(g_1 - g_0)) = a(\varepsilon - 1)^2 + b(\varepsilon - 1) + c$. This yields

$$\int_{\varepsilon}^1 \frac{C(g_0 + z(g_1 - g_0))}{z\sqrt{1-z}} dz \approx \int_{\varepsilon}^1 \frac{\tilde{C}(z)}{z\sqrt{1-z}} dz = (a + c - b) \ln \left(\frac{1 + \sqrt{1-\varepsilon}}{1 - \sqrt{1-\varepsilon}} \right) + \frac{2}{3}(3b - 4a + a\varepsilon)\sqrt{1-\varepsilon}. \quad (4.24)$$

Last, we expand in ε , giving the simple approximate formula

$$\begin{aligned} \ell_s/(2R) \approx \sqrt{\frac{k(k+1)}{6}} & \left(C(g_0) \ln(4/\varepsilon - 2) - \frac{2}{3}C(g_0) \frac{g_1 + 3g^* - 4g_0}{g^* - g_0} \right. \\ & \left. + \frac{2}{3}C(g_1) \frac{2g_1 + g_0 - 3g^*}{g_1 - g^*} + \frac{2}{3}C(g^*) \frac{(g_1 - g_0)^2}{(g^* - g_0)(g_1 - g^*)} \right) \end{aligned} \quad (4.25)$$

where

$$C(g_1) = \frac{g_1(g_0)^{k/2}}{\sqrt{k(k+1)g_0^k + (k-1)g_1(g_0) - (k+1)g_0}}, \quad (4.26)$$

$$C(g^*) = \frac{g^{*(k-1)/2}(g^* - g_0)\sqrt{g_1(g_0) - g^*}}{\sqrt{g_1(g_0) - g_0}\sqrt{(g^* - g_0)^2 + kg_0^k(g^* - g_0) - g^*(g^{*k} - g_0^k)}}, \quad (4.27)$$

$$C(g_0) = \frac{g_0^{(k-1)/2}}{\sqrt{1 - (g_0/g^*)^{k-1}}}, \quad (4.28)$$

with $g_1 = g_1(g_0)$ being determined in terms of g_0 by the algebraic equation (3.20). This formula (4.25) for the physical width of a solitary wave is good for $\varepsilon \lesssim 1/20$.

The impulse, height, and width properties are shown in Fig. 2 for the explicit solitary wave solutions presented in section 3.1.

4.2. Physical properties of the compacton. The physical form for the compacton (3.46) is given by

$$v(x - vt) = \left(\frac{1}{2}(\nu/c)^2 k(k+1) \right)^{1/(k-1)} \cos \left((x - vt)/\rho \right)^{2/(k-1)} \Theta \left(\frac{\pi}{2} - |x - vt|/\rho \right) \quad (4.29)$$

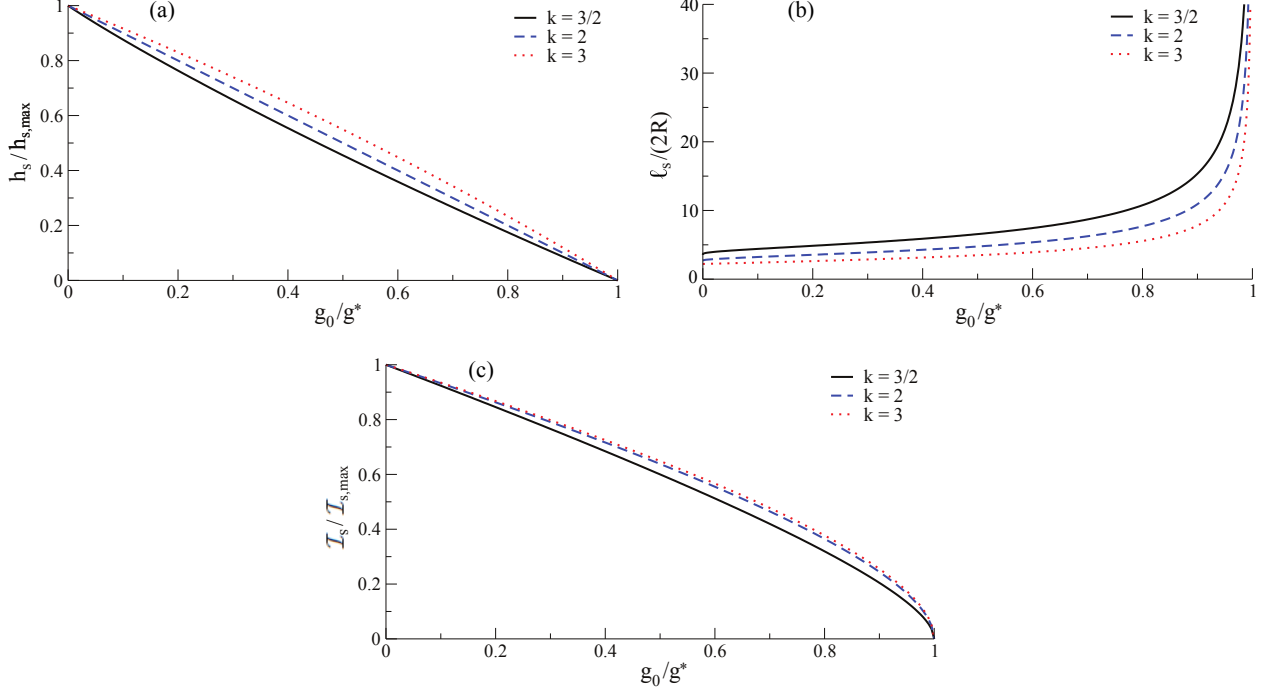


FIGURE 2. Height, width, and impulse for solitary waves with $k = \frac{3}{2}, 2, 3$

with

$$\rho = \frac{\sqrt{2k(k+1)}}{\sqrt{3(k-1)}}R \quad (4.30)$$

where $\Theta(z)$ denotes the Heaviside step function. Note the strain $v(x - \nu t)$ vanishes for $|x - \nu t| \geq \rho\pi/2$. Recall, as discussed in section 3.1, the compacton is an actual solution of the continuum system only for $1 < k < \frac{5}{3}$, since the cutoff imposed by the step function lacks sufficient differentiability when $k \geq \frac{5}{3}$.

More specifically, at the cutoff $|x - \nu t| = \rho\pi/2$, we see $v'(x - \nu t)$ is discontinuous when $k \geq 3$; $v''(x - \nu t)$ is discontinuous when $k \geq 2$; and $v'''(x - \nu t)$ is discontinuous when $k \geq \frac{5}{3}$. Higher-order differentiability does not need to be considered because when $v(x - \nu t)$ is three-times differentiable, the strain relation (2.10) shows that the displacement $U(x - \nu t)$ in the continuum system will be four-times differentiable as needed to satisfy the fourth-order LWHC wave equation (2.16).

In the same way as for solitary waves, the physical height, h_c , of the compacton is measured by the peak amplitude of the strain v relative to the asymptotic strain $v_0 = 0$. The peak strain is clearly $v_1 = (\frac{1}{2}(\nu/c)^2 k(k+1))^{1/(k-1)} = (|\nu|/c)^{2/(k-1)}/g^*$. Hence, the compacton has the height

$$h_c = (|\nu|/c)^{2/(k-1)}/g^* = H_c(\nu) \quad (4.31)$$

which is a function of ν .

Similarly, the physical width, ℓ_c , of the compacton can be measured by finding the position $|\zeta|$ at which the height $v(\zeta)$ is a fraction $0 < \varepsilon < 1$ of h :

$$v(\zeta) = \varepsilon h. \quad (4.32)$$

This gives $|\zeta|/\rho = \arccos(\varepsilon^{(k-1)/2})$, from which we can obtain the width $\ell_c = 2|\zeta|$. Hence, we obtain the formula

$$\ell_c/(2R) = \frac{\rho}{R} \arccos(\varepsilon^{(k-1)/2}) \quad (4.33)$$

yielding the width as a function of the fraction $0 < \varepsilon < 1$, which we are free to choose. Since v is zero for $|\zeta| > \ell/2$, the most natural choice would be $\varepsilon = 0$. However, for solitary waves, $\varepsilon = 0$ yields $\ell = \infty$, and so we will instead take $\varepsilon \lesssim \frac{1}{100}$ for comparison purposes. An expansion of the width formula (4.33) in ε yields

$$\ell_c/(2R) \approx (\rho/R) \left(\frac{\pi}{2} - \varepsilon^{(k-1)/2} \right). \quad (4.34)$$

Finally, the impulse integral (4.3) is easily evaluated for the compacton, giving

$$\mathcal{I}_c(\nu) = KRc^{2/(1-k)} \operatorname{sgn}(\nu) |\nu|^{(k+1)/(k-1)} \quad (4.35)$$

where $K = \frac{2\sqrt{\pi}}{\sqrt{3}}(1/g^*)^{(k+1)/2} \Gamma(\frac{k+1}{2k-2}) / \Gamma(\frac{1}{k-1})$ is a constant depending only on k . Note the impulse is a function of the wave speed ν , which is arbitrary. As a consequence, if we consider fixing the value of the impulse, then this fixes the wave speed. Physically, specifying the impulse imparted to a continuum system with no pre-compression, $v_0 = 0$, determines a unique compacton wave.

4.3. Differences between the compacton and the solitary wave family. We will now compare the physical properties of the compacton and the solitary wave family, with the impulse being fixed.

Consider specifying the value for the physical impulse $\mathcal{I} = \mathcal{I}_0$ imparted to a continuum system (such that the impulse produces a localized pulse). If the system has no pre-compression, then the impulse produces a compacton (4.29), with $\mathcal{I}_0 = KRc^{2/(1-k)} \operatorname{sgn}(\nu_c) |\nu_c|^{(k+1)/(k-1)}$ where ν_c is the speed of the compacton. The magnitude of the impulse determines the compacton speed:

$$|\nu_c| = (KR)^{(1-k)/(k+1)} c^{2/(k+1)} |\mathcal{I}_0|^{(k-1)/(k+1)} \quad (4.36)$$

In contrast, if the system has a non-zero pre-compression, then the impulse produces a solitary wave (4.6), with $\mathcal{I}_0 = \frac{2}{\sqrt{3}}(1/g^*)^{(k+1)/2} Rc^{2/(1-k)} \operatorname{sgn}(\nu_s) |\nu_s|^{(k+1)/(k-1)} \mathcal{C}((c/|\nu_s|)^{2/(k-1)} v_0 g^*)$ where ν_s is the speed of the solitary wave and where v_0 is the asymptotic strain in the system. Taking the ratio of these two expressions for \mathcal{I}_0 , we obtain the relationship

$$|\nu_c/\nu_s| = (\mathcal{C}(g_0)/\mathcal{C}(0))^{(k-1)/(k+1)} \quad (4.37)$$

in terms of g_0 which is related to v_0 by equation (4.8). The property $\mathcal{C}(0) > \mathcal{C}(g_0)$ for $g_0 > 0$ then yields

$$|\nu_c| < |\nu_s|. \quad (4.38)$$

This shows that the compacton is strictly slower than a solitary wave having the same impulse.

Furthermore, the relationship shows that a fixed impulse \mathcal{I}_0 , or equivalently a fixed compacton speed ν_c , does not determine a unique solitary wave. In particular, for any chosen speed $|\nu_s| > |\nu_c|$, the relation $\mathcal{C}(g_0) = r^{(k+1)/(k-1)} \mathcal{C}(0)$ with $r = |\nu_c/\nu_s| < 1$ can be inverted to obtain $g_0 = g_0(r) > 0$ which is the parameter controlling the profile of the resulting solitary wave. By using the approximate formula (4.13) for $\mathcal{C}(g_0)$, we find

$$g_0(r) \approx \left(1 - r^{(k+1)/(k-1)} / a + \frac{1}{2} (b/a)^2 \left(\sqrt{1 + 4r^{(k+1)/(k-1)} a/b^2} - 1 \right) \right) g^* \quad (4.39)$$

where $a = g^* \tilde{K} - 1$ and $b = 2 - g^* \tilde{K}$, with \tilde{K} given by expression (4.16). Note this formula yields $g_0(0) \approx g^*$ and $g_0(1) \approx 0$, which agrees with the exact properties $g_0 \rightarrow g^*$ when $|\nu_s| \rightarrow \infty$ and $g_0 \rightarrow 0$ when $|\nu_s| \rightarrow \nu_c$. From $g_0(r)$, we can obtain $g_1(r)$ by using the algebraic equation (3.20), and then we can evaluate the integral (4.6) with v_1 given by expression (4.7) in terms of $g_1(r)$, which yields the solitary wave $v(x - \nu t)$.

The profile of the solitary wave is sensitive to the value of the speed ratio $0 < r < 1$. When r is close to 1, the solitary wave profile is close to the compacton profile, as shown in Fig. 3(a) to Fig. 5(a) for $k = \frac{3}{2}, 2, 3$ with $r = 0.995$.

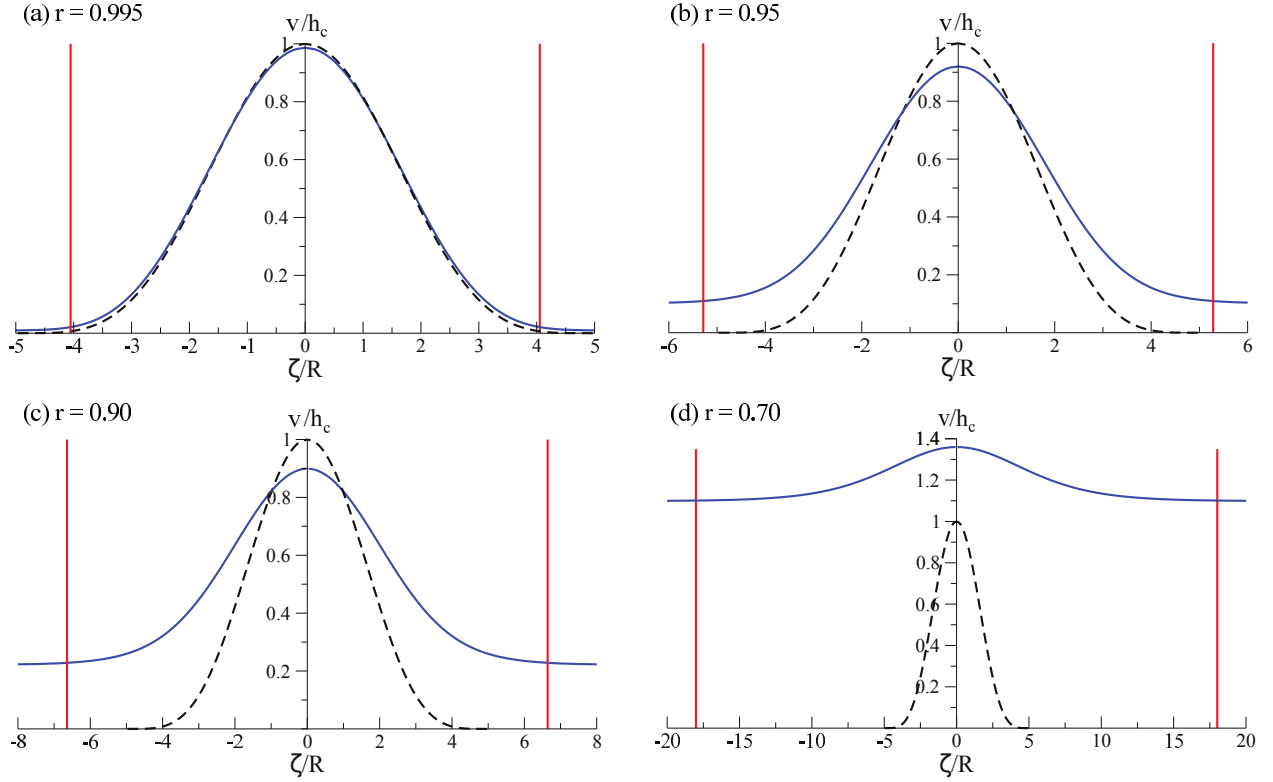


FIGURE 3. Solitary waves with $k = \frac{3}{2}$ and speed ratios $r = 0.995, 0.95, 0.9, 0.7$, shown as solid lines. Dashed lines are the compacton solution for $k = \frac{3}{2}$, and vertical lines indicate the width of the solitary wave.

As r decreases, the solitary wave profile becomes noticeably different than the compacton profile and has a smaller height and larger width. These features are shown in Fig. 3(b,c) to Fig. 5(b,c) for $k = \frac{3}{2}, 2, 3$ with $r = 0.95, 0.9$, corresponding to the speed of solitary wave being 1.05 and 1.1 times the speed of the compacton, respectively. In particular, in the case $k = \frac{3}{2}$, the width of the solitary wave is 40% larger than the compacton width and the height of the solitary wave is 40% smaller than the compacton height when their speed ratio is 1.1.

For $r \approx 0.7$, corresponding to the speed of solitary wave being 1.5 times the speed of the compacton, the solitary wave has more than twice the width of the compacton, and less than one-half of the height, which is shown in Fig. 3(d) to Fig. 5(d) for $k = \frac{3}{2}, 2, 3$.

The ratios of the solitary wave height to the compacton height, and the solitary wave width to the compacton width, are shown as a function of r in Fig. 6 for $k = \frac{3}{2}, 2, 3$. We see

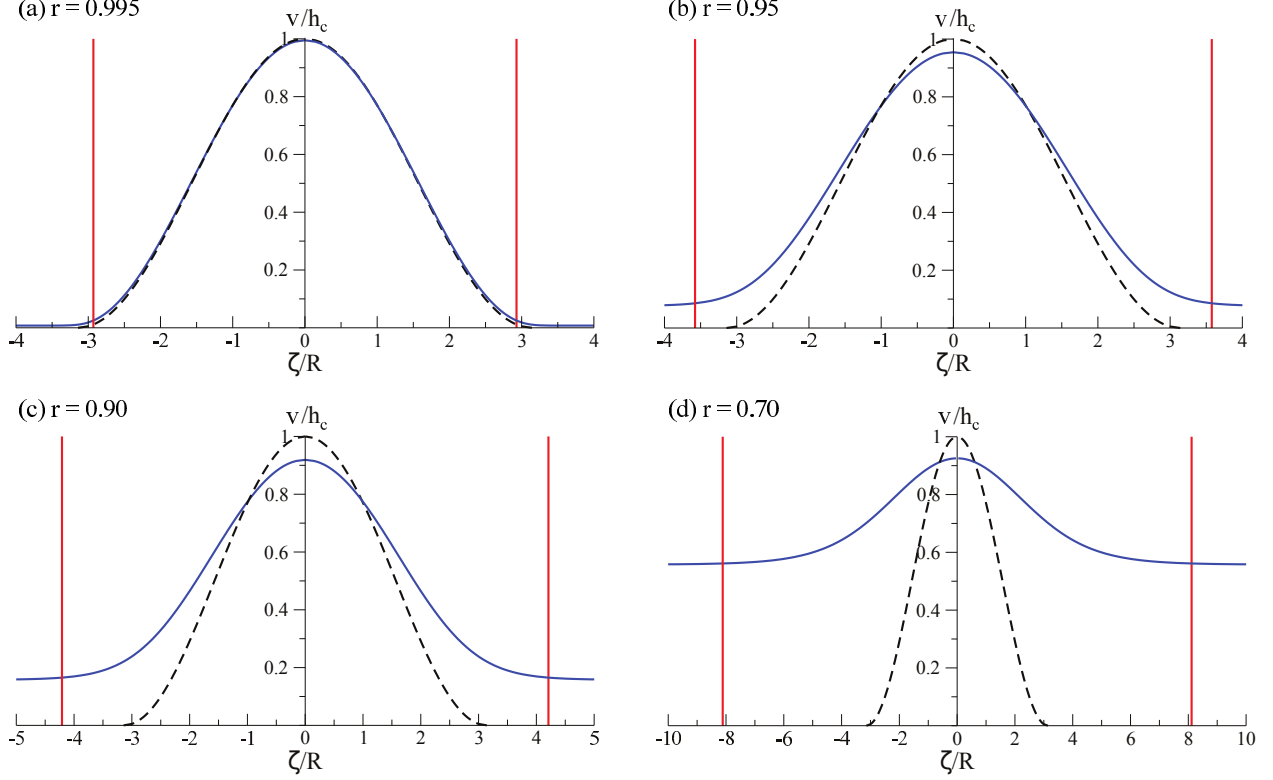


FIGURE 4. Solitary waves with $k = 2$ and speed ratios $r = 0.995, 0.95, 0.9, 0.7$. Dashed lines are the compacton solution for $k = 2$, and vertical lines indicate the width of the solitary wave.

that the height ratio reaches the value $\approx 1/2$ when the speed of the solitary wave exceeds the speed of the compacton by approximately 20% for $k = \frac{3}{2}$, 30% for $k = 2$, and greater than 40% for $k = 3$. Similarly, the width ratio reaches the value ≈ 2 when the speed of the solitary wave exceeds the speed of the compaction by approximately 15% for $k = \frac{3}{2}$, 25% for $k = 2$, and greater than 40% for $k = 3$.

Taken together, these results clearly establish that the compacton is a poor approximation to the actual solitary waves in a pre-compressed continuum system when solitary waves with speeds larger than 10% of the compacton speed are considered. Conversely, the compacton will only be a good approximation for solitary waves with speeds slightly exceeding the compacton speed. In particular, in the case $k = \frac{3}{2}$, for the width and height of solitary waves to be within 10% compared to the compacton, the speed ratio must be approximately less than 2%. See Fig. 7.

It is worthwhile to observe that the asymptotic strain, v_0 , in the continuum system is determined from expression (4.8) by $g_0(r)$ and $|\nu_s| = |\nu_c|/r$. The approximate formula (4.39) for $g_0(r)$, combined with relations (4.8) and (4.36), yields

$$v_0(r) \approx (|\mathcal{I}_0|/(KRc))^{2/(k+1)} \left(r^{2/(1-k)} \left(1 + \frac{1}{2}(b/a)^2 \left(\sqrt{1 + 4r^{(k+1)/(k-1)} a/b^2} - 1 \right) \right) - r/a \right) \quad (4.40)$$

which is a function of r , where $a = g^* \tilde{K} - 1$, $b = 2 - g^* \tilde{K}$, $K = \frac{4\pi}{\sqrt{3}} g^{*(1-k)/2} / ((k-1)\tilde{K})$, with \tilde{K} given by expression (4.16). The asymptotic strain is non-zero and increases as the speed

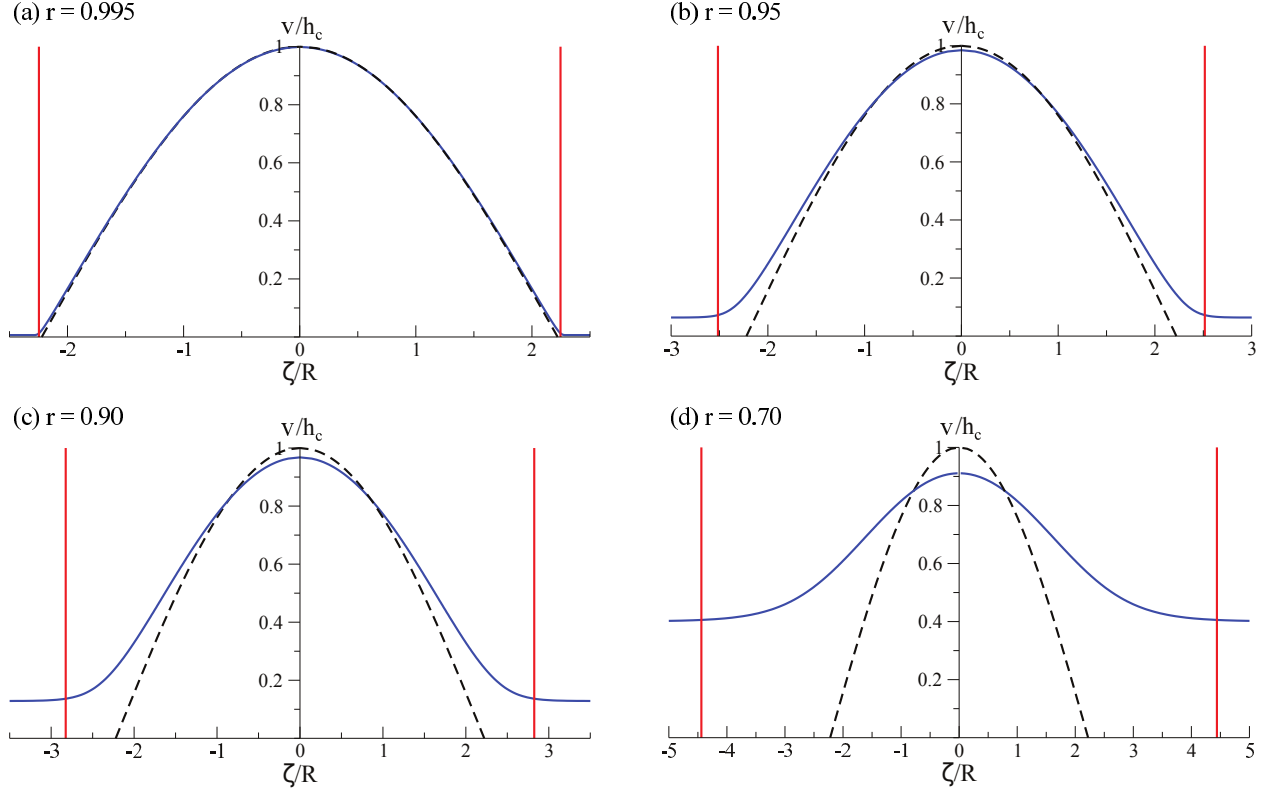


FIGURE 5. Solitary waves with $k = 3$ and speed ratios $r = 0.995, 0.95, 0.9, 0.7$. Dashed lines are the compacton solution for $k = 3$, and vertical lines indicate the width of the solitary wave.

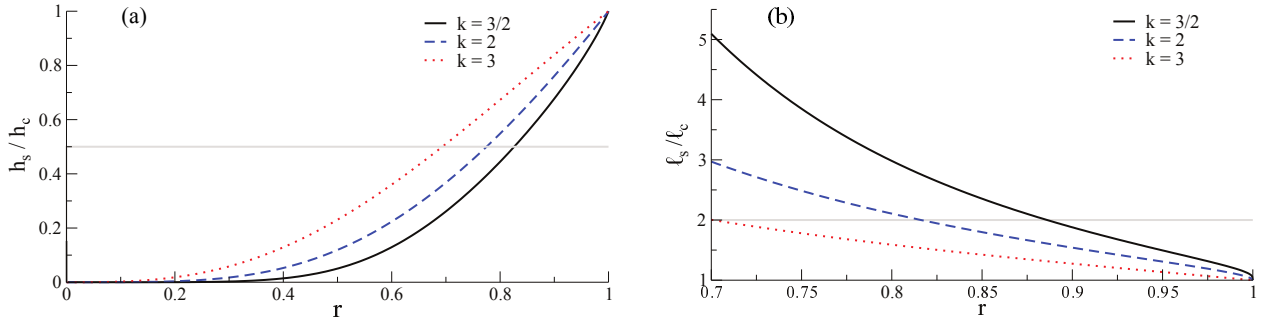


FIGURE 6. Height and width ratios for $k = \frac{3}{2}, 2, 3$ for a range of speed ratios.

ratio r decreases. Its size scales like

$$v_0(r) \propto (|\mathcal{I}_0|/(Rc))^{2/(k+1)} \quad (4.41)$$

which can be made arbitrarily small by a suitable adjustment of the material properties of the continuum system and of the magnitude of the impulse (namely, the values of the physical constants c , R , and $|\mathcal{I}_0|$). Consequently, any speed ratio $0 < r < 1$ is, in principle, physically compatible with a small pre-compression for the continuum system.

For speed ratios r close to 1, the asymptotic strain (4.40) expressed as a ratio in terms of the peak strain (4.7) is given by

$$v_0(r)/v_1(r) \approx (1-r)\hat{K} \quad (4.42)$$

where $\hat{K} = \frac{k+1}{\sqrt{\pi}}\Gamma(\frac{k+1}{2k-2})/\Gamma(\frac{1}{k-1})$ is a constant depending only on k . In the case $k = \frac{3}{2}$, this ratio is approximately 4% when the speed ratio is $r = 1.02$, which is the upper limit for the compacton to be a good approximation to the actual solitary waves.

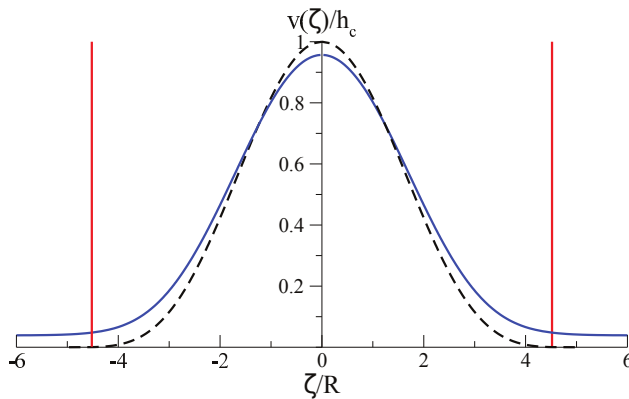


FIGURE 7. Solitary wave with $k = \frac{3}{2}$ and speed ratio $r = 0.98$, shown as the solid line. The compacton solution for $k = \frac{3}{2}$ is shown as the dashed line, and vertical lines indicate the width of the solitary wave.

5. CONCLUDING REMARKS

There are several important conclusions arising from our physical analysis of the properties of long wavelength solitary waves in the continuum model of weakly pre-compressed Hertzian chains.

The approximate formula we have derived for the physical width of solitary waves shows that all solitary waves have a width of at least four particle diameters when the chain is composed of spherical particles. This result confirms the validity of the continuum model for studying solitary waves.

Solitary waves having a fixed impulse momentum comprise a one-parameter family depending on the background strain in the chain. The background strain value determines the speed of the wave, and we obtain an explicit formula for this relationship. The shape of these solitary waves is highly sensitive to their speed.

We find that the solitary waves can be closely approximated by Nesterenko's compacton when the ratio of the background strain to the peak strain in the chain is less than 4%.

The same conclusions will hold for physical discrete systems in the long wavelength regime when $1 < k \lesssim 3.5$.

ACKNOWLEDGMENTS

S.C.A. is supported by an NSERC research grant. M.P. is supported by a Vanier Canada Graduate Scholarship from NSERC.

APPENDIX

Here we outline the main steps in the derivation of the solitary wave solution (3.28) for $k = \frac{3}{2}$, starting from the general integral expression (3.21) which is given by

$$\pm \int_g^{g_1} \frac{g^{1/4}}{\sqrt{(g - g_0)^2 + \frac{3}{2}g_0^{3/2}(g - g_0) - g(g^{3/2} - g_0^{3/2})}} dg = \xi \quad (5.1)$$

As shown in Ref. [62], the change of variable $g = h^2$ brings this integral (5.1) to the form of an elliptic integral

$$\pm 2 \int_h^{h_1} \frac{h^2}{(h - h_0)\sqrt{B(h)}} dh = \xi \quad (5.2)$$

where

$$B(h) = h\left(1 - \frac{3}{2}h_0\right)h_0^2 + (2 - 3h_0)h_0h + (1 - 2h_0)h^2 - h^3 \quad (5.3)$$

is a quartic polynomial. It is straightforward to show that this polynomial factorizes $B(h) = B_1(h)B_2(h)$ with $B_1(h) = h(h_1 - h)$ and $B_2(h) = (h + h_2)^2 + h_3^2$, where h_1, h_2, h_3 are given by expressions (3.39)–(3.41). Standard methods [64, 66] can now be used to evaluate the elliptic integral (5.2) explicitly.

The first step is to change variables by applying a linear fractional transformation

$$y = (h - y_+)/ (h - y_-), \quad (5.4)$$

with y_{\pm} being defined by the condition $B_1(h) - \lambda_{\pm}B_2(h) = -(1 + \lambda_{\pm})(h - y_{\pm})^2$, where λ_{\pm} are the roots of the discriminant of $B_1(h) - \lambda B_2(h)$. This leads to the expressions

$$(y - 1)^2 R B_1(h) = \sqrt{PQ} Y_1(y), \quad (y - 1)^2 R B_2(h) = \sqrt{PQ} Y_2(y) \quad (5.5)$$

given in terms of the quadratic polynomials

$$Y_1(y) = K_-^2 - K_+^2 y^2, \quad Y_2(y) = (K_+^2 - R)y^2 + R - K_-^2. \quad (5.6)$$

where

$$K_{\pm} = \sqrt{Q} \pm \sqrt{P} \quad (5.7)$$

and

$$P = h_2^2 + h_3^2 = B_2(0), \quad Q = (h_1 + h_2)^2 + h_3^2 = B_2(h_1), \quad R = (h_1 + 2h_2)^2. \quad (5.8)$$

Carrying out the change of variable (5.4), and splitting up the integral into terms with even/odd parity under $y \rightarrow -y$, we get

$$\int_h^{h_1} \frac{h^2 dh}{(h - h_0)\sqrt{B(h)}} = c_1 I_1 + c_2 I_2 + c_0 J_0 + c_1 J_1 + c_2 y_0 J_2, \quad (5.9)$$

where

$$I_1 = \int_y^{y_1} \frac{y dy}{(y^2 - 1)\sqrt{Y_1(y)Y_2(y)}}, \quad I_2 = \int_y^{y_1} \frac{y dy}{(y^2 - y_0^2)\sqrt{Y_1(y)Y_2(y)}}, \quad (5.10)$$

$$J_0 = \int_y^{y_1} \frac{dy}{\sqrt{Y_1(y)Y_2(y)}}, \quad J_1 = \int_y^{y_1} \frac{dy}{(y^2 - 1)\sqrt{Y_1(y)Y_2(y)}}, \quad J_2 = \int_y^{y_1} \frac{dy}{(y^2 - y_0^2)\sqrt{Y_1(y)Y_2(y)}} \quad (5.11)$$

and

$$c_0 = \frac{y_-^2(y_0 - 1)R}{\sqrt{PQ}}, \quad c_1 = -\frac{(y_+ - y_-)^2 R}{\sqrt{PQ}}, \quad c_2 = \frac{h_0^2(y_0 - 1)^2 R}{\sqrt{PQ}}, \quad (5.12)$$

with

$$y_{\pm} = \sqrt{P}(\pm\sqrt{Q} - \sqrt{P})/\sqrt{R} \quad (5.13)$$

and

$$y_1 = (h_1 - y_+)/ (h_1 - y_-) = K_- / K_+, \quad (5.14)$$

$$y_0 = (h_0 - y_+)/ (h_0 - y_-) = \frac{h_0\sqrt{R} - K_- \sqrt{P}}{h_0\sqrt{R} + K_+ \sqrt{P}}. \quad (5.15)$$

We note that the integral (5.9) must diverge to ∞ when $h \rightarrow h_0$, since this limit corresponds to the tail of the solitary wave $|\xi| \rightarrow \infty$. In terms of the variable y , this divergence occurs for $y \rightarrow y_0$.

The five separate integrals (5.10)–(5.11) can be simplified by a further change of variables. We introduce

$$z = y/y_1, \quad (5.16)$$

and let

$$\tau = K_- \sqrt{R - K_-^2}, \quad (5.17)$$

$$k = y_1^2(K_+^2 - R)/(R - K_-^2), \quad n = (y_1/y_0)^2, \quad m = y_1^2. \quad (5.18)$$

Note $y \rightarrow y_0$ now corresponds to $z \rightarrow y_0/y_1 = 1/\sqrt{n}$.

The first two integrals (5.10) can be evaluated directly in terms of elementary functions:

$$\begin{aligned} \frac{\tau}{y_1^2} I_1 &= \int_z^1 \frac{z dz}{(y_1^2 z^2 - 1) \sqrt{(1 - z^2)(1 + kz^2)}} \\ &= \frac{-1}{2\sqrt{(1 - m)(k + m)}} \left(\frac{\pi}{2} + \arctan \left(\frac{(m - 1)(1 + kz^2) + (k + m)(1 - z^2)}{2\sqrt{(k + m)(1 - m)} \sqrt{(1 - z^2)(1 + kz^2)}} \right) \right), \end{aligned} \quad (5.19)$$

and

$$\begin{aligned} \frac{y_0^2 \tau}{y_1^2} I_2 &= \int_z^1 \frac{z dz}{((y_1/y_0)^2 z^2 - 1) \sqrt{(1 - z^2)(1 + kz^2)}} \\ &= \frac{1}{2\sqrt{(n - 1)(k + n)}} \ln \left(\frac{(\sqrt{n - 1} \sqrt{1 + kz^2} + \sqrt{k + n} \sqrt{1 - z^2})^2}{(k + 1)(nz^2 - 1)} \right). \end{aligned} \quad (5.20)$$

For $z \rightarrow y_0/y_1 = 1/\sqrt{n}$, the integral I_1 is finite, while the integral I_2 has a logarithmic singularity $(y_0/y_1)^2 \tau I_2 \rightarrow \frac{-1}{2\sqrt{(n - 1)(k + n)}} \ln(nz^2 - 1) \rightarrow +\infty$.

The remaining three integrals (5.11) can be evaluated in terms of Jacobi elliptic functions:

$$\frac{\tau}{y_1} J_0 = \int_z^1 \frac{dz}{\sqrt{(1-z^2)(1+kz^2)}} = \frac{1}{\sqrt{1+k}} \operatorname{cn}^{-1}(z|l), \quad (5.21)$$

$$\frac{\tau}{y_1} J_1 = \int_z^1 \frac{dz}{(y_1^2 z^2 - 1) \sqrt{(1-z^2)(1+kz^2)}} = \frac{1}{(m-1)\sqrt{1+k}} \Pi\left(\frac{m}{m-1}; \operatorname{cn}^{-1}(z|l)|l\right), \quad (5.22)$$

$$\frac{\tau y_0^2}{y_1} J_2 = \int_z^1 \frac{dz}{((y_1/y_0)^2 z^2 - 1) \sqrt{(1-z^2)(1+kz^2)}} = \frac{1}{(n-1)\sqrt{k+1}} \Pi\left(\frac{n}{n-1}; \operatorname{cn}^{-1}(z|l)|l\right), \quad (5.23)$$

with

$$l = k/(1+k). \quad (5.24)$$

For $z \rightarrow y_0/y_1 = 1/\sqrt{n}$, the integrals J_0 and J_1 are finite, while the integral J_2 can be shown to have a logarithmic singularity.

The next step consists of extracting the singular part of J_2 by using the elliptic function identity [66]

$$\Pi(N; \theta|l) = -\Pi(l/N; \theta|l) + \theta + \frac{1}{2}\psi \ln \left(\frac{\psi + \operatorname{sn}(\theta|l)/(\operatorname{cn}(\theta|l) \operatorname{dn}(\theta|l))}{\psi - \operatorname{sn}(\theta|l)/(\operatorname{cn}(\theta|l) \operatorname{dn}(\theta|l))} \right), \quad N > 1, \quad (5.25)$$

where $\psi = \frac{1}{\sqrt{(N-1)(1-l/N)}}$. This gives

$$\begin{aligned} \Pi(n/(n-1); \operatorname{cn}^{-1}(z|l)|l) &= \operatorname{cn}^{-1}(z|l) - \Pi(l(n-1)/n; \operatorname{cn}^{-1}(z|l)|l) \\ &\quad + \frac{1}{2}\psi \ln \left(\frac{\tilde{\psi} + \sqrt{1-z^2}/(z\sqrt{1+kz^2})}{\tilde{\psi} - \sqrt{1-z^2}/(z\sqrt{1+kz^2})} \right) \end{aligned} \quad (5.26)$$

with $\tilde{\psi} = \frac{\psi}{\sqrt{k+1}} = \frac{\sqrt{1-1/n}}{(1/\sqrt{n})\sqrt{1+k/n}}$. In the logarithm term in expression (5.26), the denominator vanishes at $z^2 = 1/n$, and so we can factorize

$$\frac{\tilde{\psi} + \sqrt{1-z^2}/(z\sqrt{1+kz^2})}{\tilde{\psi} - \sqrt{1-z^2}/(z\sqrt{1+kz^2})} = \frac{(n-1)(z\sqrt{1+kz^2} + (1/\tilde{\psi})\sqrt{1-z^2})^2}{(nz^2-1)(1+kz^2 + (k/n)(1-z^2))}. \quad (5.27)$$

Thus, we can write

$$J_2 = J_{2,0} + J_{2,1} + I_3, \quad (5.28)$$

where

$$\frac{\tau y_0^2}{y_1} J_{2,0} = \frac{1}{(n-1)\sqrt{k+1}} \operatorname{cn}^{-1}(z|l), \quad \frac{\tau y_0^2}{y_1} J_{2,1} = \frac{-1}{(n-1)\sqrt{k+1}} \Pi(l(n-1)/n; \operatorname{cn}^{-1}(z|l)|l), \quad (5.29)$$

are finite for $z \rightarrow y_0/y_1 = 1/\sqrt{n}$, and where

$$\frac{\tau y_0^2}{y_1} I_3 = \frac{\sqrt{n}}{2\sqrt{k+n}} \ln \left(\frac{(n-1)(z\sqrt{1+kz^2} + (1/\tilde{\psi})\sqrt{1-z^2})^2}{(nz^2-1)(1+kz^2 + (k/n)(1-z^2))} \right). \quad (5.30)$$

has the logarithmic singularity $(y_0^2/y_1)\tau I_3 \rightarrow \frac{-\sqrt{n}}{2\sqrt{k+n}} \ln(nz^2-1) \rightarrow +\infty$.

All of the integrals (5.19), (5.20), (5.21), (5.22), (5.29), and (5.30) can be written explicitly in terms of h through the relations

$$z = y/y_1 = \frac{K_+ h - \sqrt{P} h_1}{K_- h + \sqrt{P} h_1}, \quad Y_1(y)/Y_2(y) = B_1(h)/B_2(h) \quad (5.31)$$

obtained by inverting the change of variables (5.4) and (5.16) and by using equations (5.4), (5.5), (5.13),

For the final step, the combined elementary integrals $c_1 I_1 + c_2(I_2 + y_0 I_3) = I(h)$ can be expressed in the form given by equation (3.29) after some simplifications using the following identities: First, from relation (5.5) evaluated at $y = y_0$ and $y = y_1$, we have

$$K_-^2 - K_+^2 y_0^2 = \frac{(y_0 - 1)^2 h_0 (h_1 - h_0) R}{\sqrt{PQ}}, \quad (5.32)$$

$$(K_+^2 - R) y_0^2 + R - K_-^2 = \frac{(y_0 - 1)^2 R S}{\sqrt{PQ}}, \quad (5.33)$$

$$(K_+^2 - R) y_1^2 + R - K_-^2 = \frac{(y_1 - 1)^2 R \sqrt{Q}}{\sqrt{P}}. \quad (5.34)$$

Next, we find

$$K_+ K_- = h_1 \sqrt{R}, \quad K_+ + K_- = 2\sqrt{Q}, \quad K_+ - K_- = 2\sqrt{P}, \quad (5.35)$$

and

$$y_+ - y_- = \frac{2\sqrt{PQ}}{\sqrt{R}}, \quad 1 - y_1 = \frac{2\sqrt{P}}{K_+}. \quad (5.36)$$

Last, we can derive

$$1 - m = \frac{4\sqrt{PQ}}{K_+^2}, \quad k + m = \frac{4\sqrt{PQ} K_-^2}{R(K_+^2 - h_1^2)}, \quad k + 1 = \frac{\sqrt{PQ}}{K_+^2 - h_1^2}, \quad (5.37)$$

$$n - 1 = \frac{R h_0 (h_1 - h_0) (1 - 1/y_0)^2}{K_+^2 \sqrt{PQ}}, \quad k + n = \frac{S K_-^2}{(K_+^2 - h_1^2) \sqrt{PQ}} \quad (5.38)$$

which yields

$$\frac{1 - z^2}{1 + kz^2} = \frac{K_+^2 - h_1^2}{h_1^2} \frac{Y_1(y)}{Y_2(y)}, \quad \frac{k + m}{1 - m} = \frac{h_1^2}{K_+^2 - h_1^2}, \quad \frac{k + n}{n - 1} = \frac{h_1^2 S}{(K_+^2 - h_1^2) h_0 (h_1 - h_0)}. \quad (5.39)$$

Similarly, the combined elliptic integrals $c_0 J_0 + c_1 J_1 + c_2 y_0 (J_{2,0} + J_{2,1}) = J(h)$ can be expressed in the form given by equation (3.33) by using the relations

$$l = \frac{k}{k + 1} = \frac{h_1^2 - K_-^2}{4\sqrt{PQ}}, \quad \frac{m}{1 - m} = \frac{K_-^2}{4\sqrt{PQ}}, \quad (5.40)$$

$$\frac{n}{n - 1} = \frac{K_-^2 \sqrt{PQ}}{R h_0 (h_1 - h_0) (1 - y_0)^2}, \quad \frac{l(n - 1)}{n} = \frac{(K_+^2 - R) h_0 (h_1 - h_0) (1 - y_0)^2}{4PQ}. \quad (5.41)$$

REFERENCES

- [1] V.F. Nesterenko, Propagation of nonlinear compression pulses in granular media, *J. Appl. Mech. and Tech. Phys.* 24(5) (1983), 733–743.
- [2] A.N. Lazaridi, V.F. Nesterenko, Observation of a new type of solitary waves in a one-dimensional granular medium. *J. Appl. Mech. Tech. Phys.* 26(3) (1985), 405–408.
- [3] V.F. Nesterenko, Solitary waves in discrete media with anomalous compressibility and similar to “sonic vacuum”, *Le Journal de Physique IV* 4(C8) (1994), 729–734.
- [4] R.S. Sinkovits, S. Sen, Nonlinear dynamics in granular columns, *Phys. Rev. Lett.* 74(14) (1995), 2686.
- [5] V.F. Nesterenko, A.N. Lazaridi, E.B. Sibiriyakov, The decay of soliton at the contact of two “acoustic vacuums”, *J. Appl. Mech. Tech. Phys.* 36(2) (1995), 166–168.

- [6] S. Sen, R.S. Sinkovits, Sound propagation in impure granular columns, *Phys. Rev. E* 54(6) (1996), 6857.
- [7] C. Coste, E. Falcon, S. Fauve, Solitary waves in a chain of beads under Hertz contact, *Phys. Rev. E* 56(5) (1997), 6104–6117.
- [8] S. Sen, M. Manciu, J.D. Wright, Solitonlike pulses in perturbed and driven Hertzian chains and their possible applications in detecting buried impurities. *Phys. Rev. E* 57(2) (1998), 2386.
- [9] A. Chatterjee, Asymptotic solution for solitary waves in a chain of elastic spheres, *Phys. Rev. E* 59(5) (1999), 5912–5919.
- [10] E. J. Hinch, S. Saint-Jean, The fragmentation of a line of balls by an impact, *Proc. R. Soc. London, Ser. A* 455(1989) (1999), 3201–3220.
- [11] J. Hong, J.-Y. Ji, H. Kim, Power laws in nonlinear granular chain under gravity, *Phys. Rev. Lett.* 82(15) (1999), 3058.
- [12] J.-Y. Ji, J. Hong, Existence criterion of solitary waves in a chain of grains. *Phys. Lett. A* 260(1) (1999), 60–61.
- [13] M. Manciu, S. Sen, A. J. Hurd, The propagation and backscattering of soliton-like pulses in a chain of quartz beads and related problems. (I). Propagation, *Physica A* 274(3) (1999), 588–606.
- [14] M. Manciu, S. Sen, A.J. Hurd, The propagation and backscattering of soliton-like pulses in a chain of quartz beads and related problems. (II). Backscattering, *Physica A* 274(3) (1999), 607–618.
- [15] S. Sen and M. Manciu, Discrete Hertzian chains and solitons, *Physica A* 268(3) (1999), 644–649.
- [16] E. Hascoët, H. J. Herrmann, Shocks in non-loaded bead chains with impurities, *Eur. Phys. J. B* 14(1) (2000), 183–190.
- [17] M. Manciu, S. Sen, A.J. Hurd, Impulse propagation in dissipative and disordered chains with power-law repulsive potentials, *Physica D* 157(3) (2001), 226–240.
- [18] V.F. Nesterenko, *Dynamics of heterogeneous materials*, Springer: New York, 2001.
- [19] S. Sen and M. Manciu, Solitary wave dynamics in generalized Hertz chains: An improved solution of the equation of motion, *Phys. Rev. E* 64(5) (2001), 056605.
- [20] A. Rosas, K. Lindenberg, Pulse dynamics in a chain of granules with friction, *Phys. Rev. E* 68(4) (2003), 041304.
- [21] A. Rosas, K. Lindenberg, Pulse velocity in a granular chain, *Phys. Rev. E* 69(3) (2004), 037601.
- [22] C. Daraio, V.F. Nesterenko, E.B. Herbold, S. Jin, Strongly nonlinear waves in a chain of Teflon beads, *Phys. Rev. E* 72 (2005), 016603.
- [23] J.M. English and R.L. Pego, On the solitary wave pulse in a chain of beads, *Proc. Amer. Math. Soc.* 133 (2005), 1763–1768.
- [24] V.F. Nesterenko, C. Daraio, E.B. Herbold, S. Jin, Anomalous wave reflection at the interface of two strongly nonlinear granular media, *Phys. Rev. Lett.* 95(15) (2005), 158702.
- [25] C. Daraio, V.F. Nesterenko, E.B. Herbold, S. Jin, Strongly nonlinear waves in a chain of polymer coated steel beads, *Phys. Rev. E* 73(026612) (2006), 1–7.
- [26] S. Job, F. Melo, A. Sokolow, S. Sen, Solitary wave trains in granular chains: experiments, theory and simulations, *Granul. Matter* 10(1) (2007), 13–20.
- [27] A. Sokolow, E.G. Bittle, S. Sen, Solitary wave train formation in Hertzian chains, *Europhys. Lett.* 77(2) (2007), 24002.
- [28] W. Zhen-Ying, W. Shun-Jin, Z. Xiu-Ming, L. Lei, Solitary wave interactions in granular media, *Chinese Phys. Lett.* 24(10) (2007), 2887.
- [29] M.A. Porter, C. Daraio, E.B. Herbold, I. Szelengowicz, P.G. Kevrekidis, Highly nonlinear solitary waves in periodic dimer granular chains, *Phys. Rev. E* 77 (2008), 015601.
- [30] S. Sen, J. Hong, J. Bang, E. Avalos, R. Doney, Solitary waves in the granular chain, *Physics Reports* 462(2) (2008), 21–66.
- [31] E.B. Herbold, J. Kim, V.F. Nesterenko, S.Y. Wang, C. Daraio, Pulse propagation in a linear and nonlinear diatomic periodic chain: effects of acoustic frequency band-gap, *Acta Mech.* 205(1-4) (2009), 85–103.
- [32] M.A. Porter, C. Daraio, I. Szelengowicz, E.B. Herbold, and P.G. Kevrekidis, Highly nonlinear solitary waves in heterogeneous periodic granular media, *Physica D* 238(6) (2009), 666–676.
- [33] A. Rosas, A.H. Romero, K. Lindenberg, Pulse propagation in a chain of o-rings with and without precompression. *Phys. Rev. E* 82(3) (2010), 031308.

- [34] F. Santibanez, R. Munoz, A. Caussarieu, S. Job, F. Melo, Experimental evidence of solitary wave interaction in Hertzian chains, *Phys. Rev. E* 84(2) (2011), 026604.
- [35] G. James, Periodic travelling waves and compactons in granular chains, *J. Nonlinear Sci.* 22(5) (2012), 813–848.
- [36] D. Khatri, D. Ngo, C. Daraio, Highly nonlinear solitary waves in chains of cylindrical particles, *Granul. Matter* 14(1) (2012), 63–69.
- [37] A. Stefanov and P. Kevrekidis, On the existence of solitary traveling waves for generalized hertzian chains, *J. Nonlin. Sci.*, 22(3) (2012), 327–349.
- [38] Y. Takato, S. Sen, Long-lived solitary wave in a precompressed granular chain, *Europhys. Lett.* 100(2) (2012), 24003.
- [39] V. Vitelli, M. van Hecke, Shocks in fragile matter, *Europhysics News* 43(6) (2012), 36–39.
- [40] D.A. Spence, Self similar solutions to adhesive contact problems with incremental loading, *Proceedings of the Royal Society of London A: Mathematical, Physical and Engineering Sciences* 305(1480) (1968), 55–80.
- [41] K.L. Johnson, *Contact Mechanics*, Cambridge, New York, 1985.
- [42] P.A. Johnson, X. Jia, Nonlinear dynamics, granular media and dynamic earthquake triggering, *Nature* 437 (2005), 871–874.
- [43] H. Hertz, Über die Berührung fester elastischer Körper, *J. Reine Angew. Math.* 92 (1882), 156–171.
- [44] M. Nakagawa, J.H. Agui, D.T. Wu, and D.V. Extramiana, Impulse dispersion in a tapered granular chain, *Granular Matter* 4(4) (2003), 167–174.
- [45] A. Sokolow, J.M. Pfannes, R.L. Doney, M. Nakagawa, J.H. Agui, and S. Sen, Absorption of short duration pulses by small, scalable, tapered granular chains, *Applied Physics Letters* 87(25) (2005), 254104.
- [46] J. Hong, Universal power-law decay of the impulse energy in granular protectors, *Physical Review Letters* 94(10) (2005), 108001.
- [47] R. Doney and S. Sen, Decorated, tapered, and highly nonlinear granular chain *Physical Review Letters* 97(15) (2006), 155502.
- [48] F. Melo, S. Job, F. Santibanez, and F. Tapia, Experimental evidence of shock mitigation in a Hertzian tapered chain. *Physical Review E* 73(4) (2006), 041305.
- [49] R.L. Doney, J.H. Agui, and S. Sen, Energy partitioning and impulse dispersion in the decorated, tapered, strongly nonlinear granular alignment: A system with many potential applications. *Journal of Applied Physics* 106(6) (2009), 064905.
- [50] A. Breindel, D. Sun, and S. Sen, Impulse absorption using small, hard panels of embedded cylinders with granular alignments, *Applied Physics Letters* 99(6) (2011), 063510.
- [51] M.A. Przedborski, T.A. Harroun, and S. Sen, Localizing energy in granular materials, *Applied Physics Letters* 107(24) (2015), 244105.
- [52] L. Vergara, Delayed scattering of solitary waves from interfaces in a granular container, *Physical Review E* 73(6) (2006), 066623.
- [53] C. Daraio, V.F. Nesterenko, E.B. Herbold, and S. Jin, Energy trapping and shock disintegration in a composite granular medium, *Physical Review Letters* 96(5) (2006), 058002.
- [54] S. Job, F. Santibanez, F. Tapia, and F. Melo, Wave localization in strongly nonlinear Hertzian chains with mass defect, *Physical Review E* 80(2) (2009), 025602.
- [55] G. Theocharis, M. Kavousanakis, P.G. Kevrekidis, C. Daraio, M.A. Porter, and I.G. Kevrekidis, Localized breathing modes in granular crystals with defects, *Physical Review E* 80(6) (2009), 066601.
- [56] G. Theocharis, N. Boechler, P.G. Kevrekidis, S. Job, M.A. Porter, and C. Daraio, Intrinsic energy localization through discrete gap breathers in one-dimensional diatomic granular crystals, *Physical Review E* 82(5) (2010), 056604
- [57] N. Boechler, G. Theocharis, S. Job, P.G. Kevrekidis, M.A. Porter, and C. Daraio, Discrete breathers in one-dimensional diatomic granular crystals, *Physical Review Letters* 104(24) (2010), 244302.
- [58] C. Daraio, V.F. Nesterenko, E.B. Herbold, and S. Jin, Tunability of solitary wave properties in one-dimensional strongly nonlinear phononic crystals. *Physical Review E* 73(2) (2006), 026610.
- [59] D. Sun, and S. Sen, Nonlinear grain-grain forces and the width of the solitary wave in granular chains: a numerical study. *Granular Matter* 15(2) (2013), 157–161.

- [60] J.D. Goddard, Nonlinear elasticity and pressure-dependent wave speeds in granular media, *Proceedings of the Royal Society of London A: Mathematical, Physical and Engineering Sciences* 430(1878) (1990), 105–131.
- [61] B.N. Persson, Contact mechanics for randomly rough surfaces, *Surface Science Reports* 61(4) (2006), 201–227.
- [62] M. Przedborski and S.C. Anco, Travelling waves and conservation laws for highly nonlinear wave equations modelling Hertz chains, arXiv: 1507.04759 math-ph (2017).
- [63] D. Sun, C. Daraio, and S. Sen, Nonlinear repulsive force between two solids with axial symmetry, *Physical Review E* 83(6) 2011, 066605.
- [64] D.F. Lawden, *Elliptic functions and applications*, Springer-Verlag, New York (1980).
- [65] A. Erdélyi, *Asymptotic expansions*, Dover Publications, Inc., New York (1956).
- [66] M. Abramowitz and I.A. Stegun, *Handbook of mathematical functions: with formulas, graphs, and mathematical tables, volume 55*, National Bureau of Standards (1964).